

# Accumulating Advantages: A New Conceptualization of Rapid Multiple Choice

Don van Ravenzwaaij<sup>1,2</sup>, Scott D. Brown<sup>1</sup>, A. A. J. Marley<sup>3,4</sup>, and Andrew Heathcote<sup>5</sup>

<sup>1</sup>School of Psychology, University of Newcastle <sup>2</sup>Faculty of Behavioral and Social Sciences, University of Groningen <sup>3</sup>Department of Psychology, University of Victoria <sup>4</sup>Institute for Choice, University of South Australia <sup>5</sup>School of Psychology, University of Tasmania

Correspondence concerning this article should be addressed to:

Don van Ravenzwaaij  
University of Groningen, Department of Psychology  
Grote Kruisstraat 2/1, Heymans Building, room 169  
9712 TS Groningen, The Netherlands  
Ph: (+31) 50 363 7021  
E-mail should be sent to d.van.ravenzwaaij@rug.nl.

## Abstract

Independent racing evidence-accumulator models have proven fruitful in advancing understanding of rapid decisions, mainly in the case of binary choice, where they can be relatively easily estimated and are known to account for a range of benchmark phenomena. Typically, such models assume a one-to-one mapping between accumulators and responses. We explore an alternative independent-race framework where more than one accumulator can be associated with each response, and where a response is triggered when a sufficient number of accumulators associated with that response reach their thresholds. Each accumulator is primarily driven by the difference in evidence supporting one vs. another response (i.e., that response’s “advantage”), with secondary inputs corresponding to the total evidence for both responses and a constant term. We use Brown and Heathcote’s (2008) LBA to instantiate the framework in a mathematically tractable measurement model (i.e., a model whose parameters can be meaningfully recovered from data). We show this “Advantage LBA” model provides a detailed quantitative account of a variety of benchmark binary and multiple choice phenomena that traditional independent accumulator models struggle with; in binary choice the effects of additive versus multiplicative changes to input values, and in multiple choice the effects of manipulations of the strength of lure (i.e., non-target) stimuli and Hick’s Law. We conclude that the Advantage LBA provides a tractable new avenue for understanding the dynamics of decisions among multiple choices.

**Keywords:** Evidence accumulation models, RT tasks, Hick’s Law, lateral inhibition, max-next.

In everyday life, we are constantly confronted with tasks that require choosing one among many options. These decisions often become more difficult as the number of alternatives increase, leading to slowed response time (RT) and decreases in choice accuracy. It is attractive to model the dynamics of such multiple-choice decisions with racing evidence-accumulation processes as such models can be applied to choosing among any number of options by simply allocating one accumulator to each option. These models assume that once the relevant information is perceptually encoded and/or extracted from memory, each accumulator accrues evidence favoring its option. The first accumulator to satisfy a stopping rule (e.g. a threshold on its evidence total) leads to the response with which it is associated. Notable recent examples include the leaky competing accumulator (LCA; Usher & McClelland, 2001), the “max-next” (Brown, Steyvers, & Wagenmakers, 2009; McClelland, Usher, & Tsetos, 2011; McMillen & Holmes, 2006), the ballistic accumulator (Brown & Heathcote, 2005), and the linear ballistic accumulator (LBA; Brown & Heathcote, 2008). The LBA model differs from the others in that accumulation, and the “stopping rule” that determines when a response is chosen, are independent for each accumulator, which makes it functionally and computationally simple, mathematically tractable, and easily extended to more complex decision paradigms (e.g., Eidels, Donkin, Brown, & Heathcote, 2010; Holmes, Trueblood, & Heathcote, 2016; Trueblood, Brown, & Heathcote, 2014).

A typical multiple-choice experiment either: 1) presents one of  $N$  possible stimuli on each trial, with each stimulus associated with a single correct response (e.g., Lacouture & Marley, 1995; Leite & Ratcliff, 2010; Pachella & Fisher, 1972), or 2) simultaneously presents  $N$  stimuli on each trial, again with each stimulus associated with a single correct response (e.g., Brown et al., 2009; Dassonville, Lewis, Foster, & Ashe, 1999; Kveraga, Boucher, & Hughes, 2002; Lee, Keller, & Heinen, 2005; ten Hoopen, Akerboom, & Raaymakers, 1982; Vickrey & Neuringer, 2000). A well-known problem in the application of independent racing accumulator models to both multiple-choice paradigms is that the conventional one-to-one mapping between stimuli and accumulators leads to *faster* decisions with more accumulators (i.e., “statistical facilitation”, Raab, 1962), whereas in practice decisions slow down. One proposed solution is to relax the assumption that accumulation is independent, as occurs in the LCA via lateral inhibitory interactions. Another is a stopping rule that depends on the moment-to-moment evidence totals in more than one accumulator, as occurs in the max-next model through requiring a minimum difference between the largest and second largest evidence totals to initiate a response. Here we explore an alternative framework, which applies to both types of multiple-choice paradigm, and which maintains independence in accumulation, but relaxes the assumption that each response is represented by only one accumulator. The stopping rule can depend on more than one accumulator, but only through threshold-crossing events, making the framework mathematically tractable.

In our proposed framework the rate of evidence accumulation for each unit is primarily based on relative rather than absolute inputs (see Marley, 1991 and Tversky & Simonson, 1993, for relative evidence models of choice probabilities, and Usher & McClelland, 2004 and Trueblood et al., 2014, for a relative-evidence model of both RT and choice). Specifically, we propose that alternatives are evaluated in pairs, so, when there are more than two alternatives, more than one accumulator is associated with each response. The input for each accumulator is a weighed sum of: (1) the difference or “advantage” in evidence for the alternative associated with the accumulator over the other alternative, (2) the total evidence

for both alternatives, and (3) a bias term (see Blavatsky, 2012, for a related formulation). Because the first term has the dominant effect we describe this as an *advantage input* scheme. We explore the mathematically tractable situation where these pairwise comparisons run independently and in parallel. When this parallel independent race model is instantiated using linear ballistic accumulators, as we do here, we call the resulting model the “Advantage LBA” (ALBA).

One new contribution of our modelling framework is the idea that a response option may be associated with more than one accumulator. This occurs when there are more than two response options, whereas when there are only two options a one-to-one mapping applies. Thus, we are able to release independent accumulator models of multiple-alternative choice from the traditional one-to-one mapping between accumulators and responses while remaining consistency with traditional approaches to binary choice. We first show that our advantage-input scheme enables good fits of the ALBA to data from a two-alternative forced-choice paradigm that have been claimed to be problematic for independent racing accumulator models but consistent with dependent accumulation as instantiated in the LCA model (Teodorescu, Moran, & Usher, 2016, Experiment 1). We then extend the two-alternative ALBA to choices among more than two response alternatives, and demonstrate that it provides good fits to data from both types of multiple-choice paradigm that are problematic for existing independent-race models. The mathematical properties of the accumulators and input scheme in the multiple-alternative ALBA are identical to those in the two-alternative ALBA, but an extension to the idea of a stopping rule is required to account for the association of each response to more than one accumulator.

A second new contribution of our work is an exploration of stopping rules. In the main body of the paper we focus on a “Win-All” stopping rule, with details of alternative stopping rules reported in supplementary materials. We report fits of the Win-All ALBA to a task requiring choice among four simultaneously presented alternatives (Teodorescu & Usher, 2013, Experiment 1a) in which effects of the relative strengths of non-target (lure) response options were best fit by the max-next model, and which were taken to be incompatible with independent accumulation. We show that the Win-All ALBA, whose stopping rule is conceptually related to the max-next stopping rule, provides an accurate and detailed account of this data. We then extend the Win-All ALBA to address a data set that exemplifies a long-standing benchmark phenomenon for multiple-choice paradigms when assigning a single stimulus into one of many classes, Hick’s Law (van Maanen et al., 2012). Hick’s Law states that the mean RT and the logarithm of the number of choice alternatives are linearly related (Hick, 1952; Hyman, 1953). We demonstrate that the Win-All ALBA naturally provides an account of Hick’s Law.

In both of the applications of the ALBA to multiple-choice data, we show that all the parameters of the Win-All ALBA are identifiable by performing parameter-recovery simulations. These successful recoveries underline a significant improvement in the utility of our approach for behavioral applications compared to non-independent race models. Non-independent models tend to be mathematically intractable, and so it is difficult to compute a key quantity required to fit them to data, their likelihood functions. Miletic, Turner, Forstmann, and Van Maanen (2017) explored a computationally intensive simulation-based method to obtain the LCA’s likelihood, but found that it was practically impossible to recover the LCA’s parameters (i.e., to accurately estimate them from fits to data). When

parameter recovery is not possible it is dangerous to interpret estimated parameter values as they may not be psychologically meaningful. For the Win-All ALBA, in contrast, we can safely interpret parameter estimates, and so we present and discuss them in each application, particularly highlighting the consistency of estimated weights for the sums and difference components of the advantage coding scheme that hold over the variety of paradigms we examine. In the next section we begin by defining this coding scheme for the simple binary-choice case.

### Advantage-input coding for binary choice

The standard LBA model for binary choice (Brown & Heathcote, 2008) has two accumulators, each of which starts from an independently sampled and uniformly distributed point between 0 and  $A_i > 0$ ,  $i = 1, 2$ , after which evidence is accumulated linearly for each response option, reflecting the assumption that stimulus input remains fixed throughout the trial. Each evidence accumulator has a drift rate  $d_i$ , and for each trial each drift rate is independently drawn from a normal distribution truncated at zero (Heathcote & Love, 2012), with means  $v_i$ , and standard deviations  $s_i$ .<sup>1</sup> Thresholds  $b_i > A_i$  determine a speed-accuracy trade off; smaller values lead to faster decisions at the cost of a higher error rate. Sometimes the same threshold and maximum starting points are assumed for both accumulators, in which case we drop the subscript. Usually, rather than directly estimating the threshold, we estimate  $B = b - A$ , the distance from the maximum starting point ( $A$ ) to the response threshold ( $b$ ), which makes it easy to fulfill the assumption that an accumulator cannot start above its threshold (i.e.,  $b > A$ ) by enforcing  $B > 0$ . Manipulations affecting a-priori plausibility of responses (say, a cue that is compatible 80% of the times, see Teodorescu & Usher, 2013) can be expected to simultaneously elevate the starting point of the compatible stimulus and depress the starting point of the incompatible stimulus.

Together, the accumulator ( $A$  and  $B$ ) and input ( $v$  and  $s$ ) parameters define a distribution of decision times,  $DT$ . Response times also include the time taken for processes such as stimulus encoding and response production, which together make up the non-decision time (Luce, 1986). We assume non-decision time is a constant,  $t_0$ , that shifts the distribution of  $DT$  such that  $RT = DT + t_0$ .

For binary choice, stimulus  $i$  has objective value  $O_i$ ,  $i = 1, 2$ . In our application, applied to the data of Experiment 1 of Teodorescu et al. (2016), the luminance (in lumens) of the visual stimuli are linear with respect to a measure (vis., MATLAB RGB values) for which 0 (resp., 1) represents the minimum (resp., maximum) screen luminance. We assume that those objective values, in the interval  $(0, 1)$ , are logarithmically transformed to subjective brightness values,  $S_i = \log(O_i)$  (Fechner, Boring, Howes, & Adler, 1966). The advantage-input rate for each accumulator is then an additive combination of the difference between the subjective brightness values,  $S_1 - S_2$  (resp.,  $S_2 - S_1$ ), with weight  $w_D$ , and their sum,  $S_1 + S_2$ , with weight  $w_S$ , plus a bias parameter,  $v_0 > 0$ ; see Equations 1 and 2 below.

To clearly differentiate this type of input scheme from that used in past applications of the standard LBA (where objective values and/or their mapping to subjective values

<sup>1</sup>The original 2008 model assumed an unbounded normal distribution. Other drift rate distributions also yield tractable models (see e.g. Terry et al., 2015), but most recent applications of the LBA assume a truncated Normal distribution.

were often not known and so rates were freely estimated) we denote the mean rate for the accumulator associated with the advantage of stimulus 1 over 2 (and hence also associated with a response favoring stimulus 1) as  $v_{1-2}$ , and similarly  $v_{2-1}$  for the other accumulator.

$$v_{1-2} = v_0 + w_D(S_1 - S_2) + w_S(S_1 + S_2) \quad (1)$$

$$v_{2-1} = v_0 + w_D(S_2 - S_1) + w_S(S_1 + S_2) \quad (2)$$

The bias parameter,  $v_0$ , can take on values that ensure that each accumulator has a non-negative drift rate and hence eventually reaches its threshold, which in turn ensures that a response is made in finite time (for a similar mechanism see e.g., Bogacz, Usher, Zhang, & McClelland, 2007; Busemeyer, Townsend, Diederich, & Barkan, 2005; van Ravenzwaaij, van der Maas, & Wagenmakers, 2012). The “difference weight”,  $w_D$ , is constrained to be non-negative and therefore the drift rate  $v_{1-2}$  (resp.,  $v_{2-1}$ ) increases (resp., decreases) as the brightness difference  $S_1 - S_2$  increases. We constrain the “sum weight”  $w_S$  to non-negative values and therefore the drift rate increases with the overall magnitude of the pair.

We describe this as an “advantage” input coding scheme as typically  $w_D \gg w_S$ , and so the difference term dominates in determining the drift rate. A large difference effect makes sense as it means the rates favor the correct response. However, a non-zero sum term is also necessary in order to account for effects of the absolute strength of the stimuli. In the framing given by Teodorescu et al. (2016), whose work inspired this formulation and whose data we fit in the next section, these rates are partially absolute but mostly relative.

Each of  $v_0$ ,  $w_S$ , and  $w_D$ , are estimated from the data, and so the units used to measure the stimuli do not matter up to a linear transformation - i.e., the stimulus measures are interval scales. We assume a common variance,  $s$ , for the drift rate distribution of all advantage accumulators within a condition, and we assume that the inputs to the accumulators are uncorrelated. An illustration of the two-alternative ALBA for a brightness identification task with two response options is given in Figure 1. In the next section, we test this model by fitting it to a data set that tests the relative influences of the sum and difference components of the inputs.

### Absolute versus Relative Input Differences

Teodorescu et al.’s (2016) Experiment 1 compared two-alternative forced choice performance in a baseline condition with luminance values of  $\{.4 \text{ vs. } .3\}$ , against performance in an “additive boost” condition, in which luminance values were elevated through the addition of 0.2 to  $\{.6 \text{ vs. } .5\}$ , and a “multiplicative boost” condition, in which they were elevated through multiplication by 1.5 to  $\{.6 \text{ vs. } .45\}$ . The two boosts were chosen such that the correct stimuli have identical objective values (.6). As a result, the additive and multiplicative conditions differ only in the luminance values of their incorrect stimuli. Although the task required a judgment about relative brightness, the authors found that both accuracy and response time were also sensitive to the absolute values of luminance relative to the baseline condition, both when the absolute value of the difference in luminance between stimuli was the same as in the baseline condition (i.e., in the additive condition) and when the ratio of luminance was the same (i.e., in the multiplicative condition; see Teodorescu et al., 2016, Figure 1c, bottom panel, see also Figure 2 of this paper). The authors attributed this pattern either to non-independent accumulation of absolute values, due to

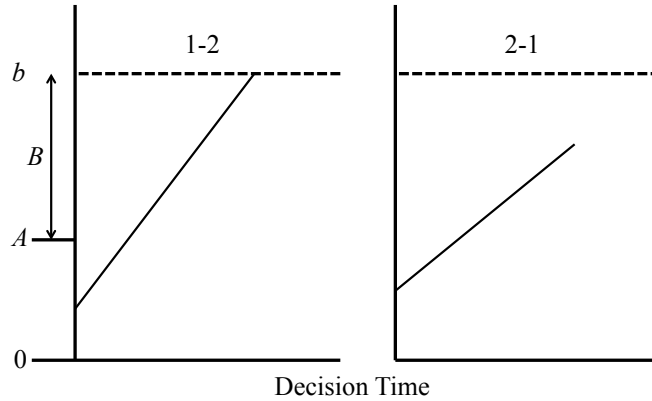


*Figure 1.* The ALBA and its parameters for a two alternative brightness identification task. Evidence accumulation begins at a start point drawn randomly from a uniform distribution on the interval  $[0, A]$ . Evidence accumulation is governed by drift rates  $d_{1-2}$  and  $d_{2-1}$ , drawn across trials from a normal distribution with means  $v_{1-2}$  and  $v_{2-1}$  and standard deviation  $s$ , truncated to positive values. A response is given as soon as one accumulator reaches the threshold  $b = A + B$ . Observed RT is an additive combination of the time during which evidence is accumulated and non-decision time  $t_0$ .

lateral inhibition as in the LCA, or independent accumulation of differences with activation dependent processing noise. Here we show that the latter mechanism can be replaced in an independent accumulation model by allowing the sum of the subjective brightness values over stimuli to have a small effect on drift rates.

In Teodorescu et al.’s (2016) experiment, each participant performed 1,200 trials, 400 in each condition, with the conditions randomly intermixed. As described in the previous section, we assumed subjective brightness to be the logarithm of the luminance values and these subjective brightness values were entered into Equations 1 and 2 to calculate drift rates. Note that the logarithmic transformation means the baseline and multiplicative conditions have equal subjective differences, which are larger than the subjective difference for the additive condition, whereas the subjective sum increase from baseline to multiplicative to additive conditions. These sum and difference values entirely account for condition effects, as the same seven estimated parameters apply to each condition: baseline drift rate ( $v_0$ ), sum ( $w_S$ ) and difference ( $w_D$ ) weights, non-decision time ( $t_0$ ), rate variability ( $s$ ), start-point variability ( $A$ ) and the right-response accumulator threshold ( $B_R$ ). The left-response accumulator threshold was fixed at  $B_L = 1$  to make the model identifiable (Donkin, Brown, & Heathcote, 2009) and different thresholds for each accumulator allowed for response bias.

Details of the estimation methods are given in subsection “B1. Estimation Details:

Table 1

Median parameter values, with a 95% credible intervals for two-alternative ALBA model fit to Teodorescu et al. (2016) Experiment 1. Rows correspond to participants (Pp), except the bottom row, which is the average of the corresponding values above).

Pp	$A$	$B_R$	$t_0$	$v_0$	$s$	$w_D$	$w_S$
1	1.38 (0.78, 2.12)	0.87 (0.80, 0.94)	0.22 (0.16, 0.27)	2.73 (2.01, 3.73)	1.39 (0.99, 1.92)	5.43 (3.52, 8.19)	0.76 (0.45, 1.25)
2	4.81 (3.40, 6.97)	1.18 (1.04, 1.37)	0.42 (0.39, 0.45)	6.56 (4.82, 9.10)	2.28 (1.65, 3.26)	11.14 (7.56, 17.18)	1.56 (0.97, 2.47)
3	1.27 (0.76, 1.86)	0.97 (0.91, 1.02)	0.17 (0.12, 0.22)	2.96 (2.24, 3.82)	1.11 (0.84, 1.46)	2.92 (2.03, 4.07)	0.33 (0.16, 0.57)
4	4.20 (3.07, 5.64)	0.90 (0.79, 1.03)	0.30 (0.28, 0.32)	7.72 (5.83, 10.21)	3.75 (2.87, 4.9)	14.31 (10.17, 20.08)	1.31 (0.60, 2.24)
5	1.87 (1.43, 2.65)	1.28 (1.19, 1.41)	0.12 (0.10, 0.17)	3.15 (2.63, 4.15)	1.26 (1.08, 1.68)	3.16 (2.52, 4.58)	0.61 (0.41, 0.95)
6	1.63 (1.19, 2.22)	1.07 (1.01, 1.14)	0.21 (0.13, 0.27)	2.05 (1.65, 2.58)	0.66 (0.51, 0.86)	2.03 (1.48, 2.84)	0.17 (0.07, 0.30)
7	2.62 (2.15, 3.16)	0.93 (0.85, 1.02)	0.10 (0.10, 0.12)	2.11 (1.81, 2.44)	0.77 (0.70, 0.85)	2.52 (2.19, 2.93)	0.35 (0.22, 0.50)
<b>Mean</b>	<b>2.54 (1.82, 3.52)</b>	<b>1.03 (0.94, 1.13)</b>	<b>0.22 (0.18, 0.26)</b>	<b>3.90 (3.00, 5.15)</b>	<b>1.60 (1.23, 2.13)</b>	<b>5.93 (4.21, 8.55)</b>	<b>0.73 (0.41, 1.18)</b>

Absolute versus Relative Input Differences” in Appendix B. Table 1 reports posterior median parameter estimates. For all participants the difference component of the rates had a much higher weight than the sum component, on average by approximately an order of magnitude, but the sum component was non-negligible. This resulted in mean rates for the target advantage accumulator of 4.06, 4.65 and 4.1 for baseline, multiplicative and additive conditions, respectively, and 0.65, 1.24 and 1.94, respectively, for the lure advantage accumulator. The small sum component does not change the equal target-lure differences in subjective brightness for baseline and multiplicative conditions (both 3.41), with a much smaller difference in the additive condition (2.16) reflecting the smaller difference in subjective brightness. However, the sum component is sufficient to account for the small absolute effects in the data.

Figure 2 shows the model fits the data well, not only in terms of accuracy and average RT but also RT distribution. The ALBA parameter estimates are consistent with Teodorescu et al.’s (2016) conclusion that accumulation is partially absolute (the sum component of the ALBA) and partially relative (the difference component of the ALBA). Our model fit is at least as good as their fit with the LCA, but a fair comparison is difficult because the LCA’s intractability makes it difficult to be sure that it has been fit in an optimal manner. Recently Ratcliff, Voskuilen, and Teodorescu (2018) showed that the Diffusion Decision Model with trial-to-trial rate variability that increases linearly with the mean rate provides a better account than the LCA of two-alternative forced-choice data displaying the same pattern of results as shown here. However, the diffusion-decision model cannot be easily generalized to multiple alternatives, whereas the ALBA can, as we show in the next section.

### The multiple-alternative ALBA

The multiple-alternative ALBA maintains the same underlying type of accumulation as the two-alternative ALBA, but decisions are made when each of a pre-specified *set* of accumulators has crossed its threshold, as opposed to a single accumulator crossing a threshold (for a similar approach see Eidels et al., 2010). The combination stopping rules may be thought of as being realized by counters, with one counter for each possible response, although there may be other interpretations (e.g., logic gates). Counts are incremented by threshold-crossing events in a set of accumulators connected to the counter. The response associated with the counter is initiated as soon as a criterion number of counts is achieved.

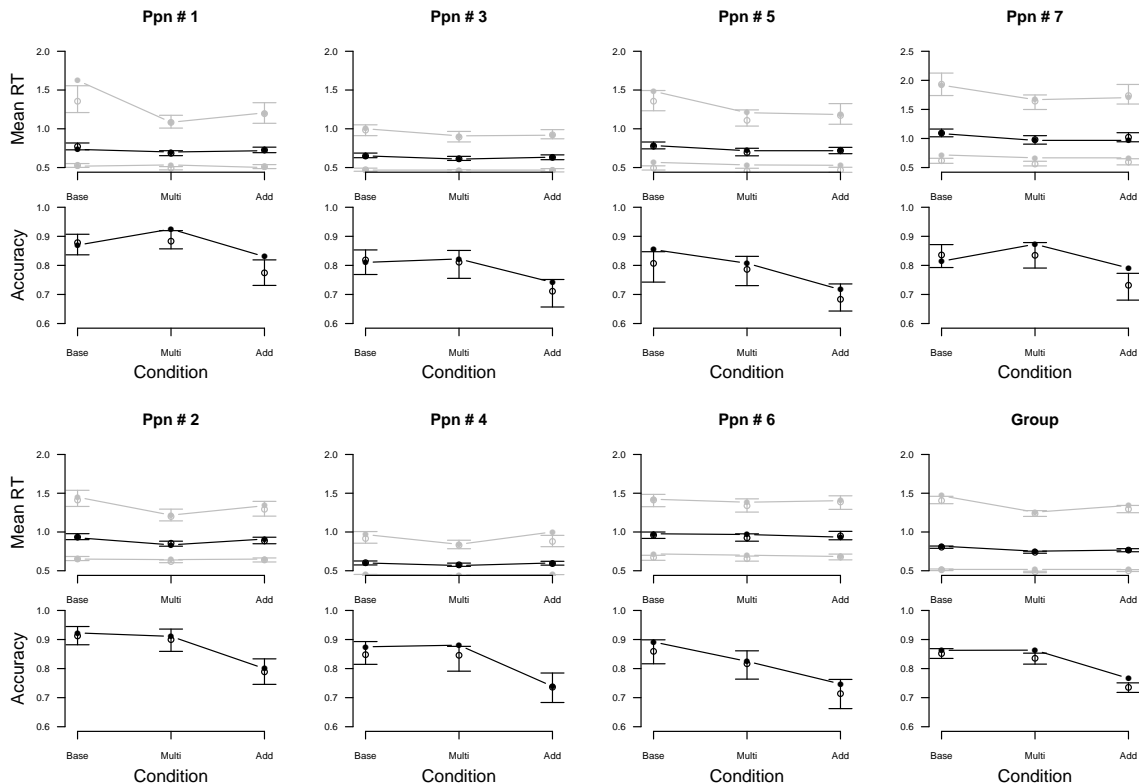


*Figure 2.* Posterior predictive data for fits to the Experiment 1 data of Teodorescu et al. (2016). RTs for the .5 (black), .1, and .9 (gray) deciles calculated for the baseline (Base), multiplicative (Mult), and additive (Add) conditions, and the proportion of correct responses for the respective conditions, both at the individual level (left three columns and top of right column) and for aggregate data (bottom right column). For all panels, error bars represent posterior predictive data simulated from model fits (the bar extends to the middle 95% of generated summary statistics, with the dot in the middle indicating the median) and lines represent data.

As an example, consider a task in which a participant has to decide which of four stimuli is the brightest: 1, 2, 3, or 4. For this decision, a standard accumulator model, such as the LBA, would assume a one-to-one mapping between accumulators and choices. This leads to four accumulators, which we denote 1, 2, 3, and 4 with corresponding drift rates  $d(1)$ ,  $d(2)$ ,  $d(3)$ , and  $d(4)$ . For the same decision, the ALBA has a total of 12 advantage accumulators, each taking as input a difference between the evidence values for an ordered pair of stimuli. We denote these accumulators: 1-2, 2-1, 1-3, 3-1, 1-4, 4-1, 2-3, 3-2, 2-4, 4-2, 3-4, and 4-3. In general for  $n$  responses there are  $n(n+1)/2$  comparisons that can be made and hence  $n(n+1)$  accumulators, half for comparisons in one direction and half for comparisons in the other direction (e.g., 1-2 vs. 2-1).

Even though the ALBA model has more accumulators than the standard LBA model, it does not require extra parameters. To illustrate, consider a trial on which stimulus



1 is brightest and the other stimuli, all less bright than stimulus 1, are equally bright to one another. In the traditional LBA, this stimulus set provides a strong “matching” subjective input value  $S_M$  to accumulator 1 and a smaller “mismatching” subjective input value of  $S_m$  to all other accumulators. In the corresponding case for the ALBA, each “matching” advantage accumulator (i.e., 1-2, 1-3, and 1-4, where the matching term is first) would have an advantage drift rate value of  $v_0 + w_D(S_M - S_m) + w_S(S_M + S_m)$ ; each “mismatching” advantage accumulator (i.e., 2-1, 3-1, and 4-1, where the matching term is second) would have an advantage drift rate value of  $v_0 + w_D(S_m - S_M) + w_S(S_M + S_m)$ ; and each of the remaining six “unrelated” accumulators (i.e., 2-3, 2-4, 3-2, 3-4, 4-2, and 4-3, where the matching term does not appear) would have an advantage drift rate value of  $v_0 + w_S(S_m + S_M)$ , as the difference term is zero. These values serve as the mean drift rates for their respective advantage accumulators.

We assume that the standard deviation for the drift rate distribution of all advantage accumulators is the same. We also assume that the inputs to all accumulators are uncorrelated. These assumptions correspond to the case where, on each trial for each accumulator, an independent random sample drawn from the same distribution is added to the mean drift rate of the accumulator.<sup>2</sup>

The mean drift rates for all advantage accumulators are determined by only three free parameters, the baseline rate,  $v_0$ , and the sum,  $w_S$ , and difference,  $w_D$ , weights. Each of the advantage accumulators has an input, and hence mean drift rate, determined by the dimensions of the stimuli (see Trueblood et al., 2014, for another approach where multiple-choice drift rates are constructed from differences). For our applications here, other standard LBA parameters  $A$ ,  $B$ , and  $t_0$  are assumed to be identical across advantage accumulators and are free parameters to be estimated from the data. However, situations likely exist where these restrictions must be relaxed. For instance, to accommodate response bias, different values of  $B$  could be allowed for the different sets of accumulators associated with each response. A lower value of  $B$  would make it quicker for accumulators in the set to finish, and hence bias responding towards the associated response. Different schemes for ensuring that some or all drift rates are positive are also possible, such as by taking the ratio rather than difference of subjective brightness values (e.g., Hawkins et al., 2014). These possibilities may have practical and conceptual advantages, but we leave their investigation to future work.

With the details of the advantage accumulators established, the last thing is to determine a stopping rule: which (set of) accumulator(s) needs to finish before a response is initiated? Here, we focus on one stopping rule, which we call Win-All, that is conceptually closest to a max-next model. We investigated two other stopping rules, Lose-All, and Lose-One, both of which are discussed in Appendix A. Note that for the two-alternative case, all these stopping rules collapse to the same end-result, as there are only two advantage accumulators.

<sup>2</sup>If the rate standard deviation was in part due to variability in each input, and that variability could differ between inputs, then only equality between advantage accumulators with the same inputs (e.g., 2-1 and 1-2) follows. However, in this case correlations would arise among accumulators that share inputs. Although this possibility is reasonable it makes the model more difficult to deal with mathematically. Systematic differences in rate variability among accumulators that are not a function of inputs do not affect tractability but were not adopted here as it did not seem necessary in our applications, but may be reasonable and necessary in other applications.

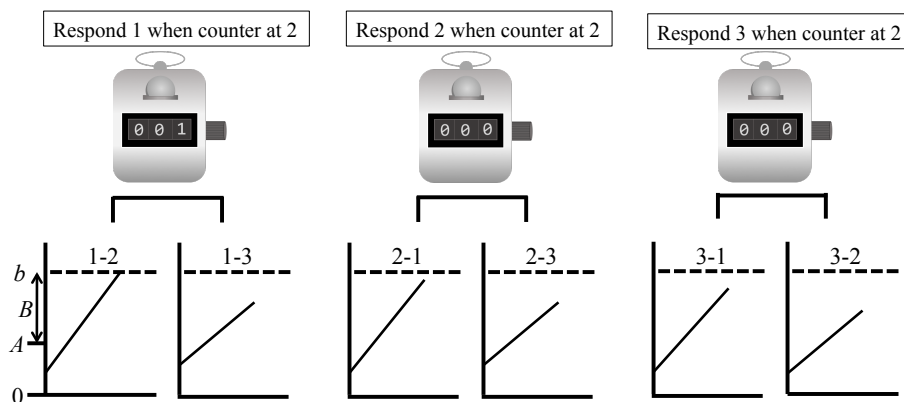


Figure 3. The Win-All version of ALBA for a three alternative task. Only the first counter to reach a count of 2 triggers a response.

### Win-All

The Win-All rule assumes that a response is made as soon as each of the accumulators associated with one of the response options has reached its threshold. For example, a Win-All rule will choose option 1 from  $\{1,2,3\}$  if and only if:

1. Accumulators 1-2 and 1-3 have reached their thresholds, and:
2. At least one of the accumulators in each of the sets  $\{2-1, 2-3\}$  and  $\{3-1, 3-2\}$  has *not* reached its threshold.

Put simply, response option 1 is chosen if it is the first option to have beaten every other response option. This rule could be instantiated by linking each response with a counter having two inputs (e.g., from 1-2 and 1-3 for a 1 response) and requiring two counts to trigger its response. An illustration for a brightness identification task with three response options is given in Figure 3.

With the Win-All rule, it is mathematically possible for accumulator termination (i.e., threshold-crossing) sequences to occur which give rise to responses in a way that appears counter intuitive. For example, the termination sequence 2-1, 3-1, 1-2, and then 1-3 would result in choosing option 1, as it is the first option to have beaten all of its competitors. This may appear counter intuitive, because option 1 has also been beaten by each of its competitors. However, with reasonable parameter settings, such sequences are exceedingly

unlikely, because they would require opposite pairs to reach threshold close together in a sequence, which will only happen if they have similar inputs. However, in this case the difference between inputs will be small, and so they are unlikely to complete early in the sequence.

Under the Win-All rule, probability of responding with choice 1 at time  $t$  is:

$$p_1(t) = \sum_{I \neq 1} \left[ PDF_{1-I}(t) \times \prod_{J \neq [1, I]} CDF_{1-J}(t) \right] \times \prod_{I \neq 1} \left[ 1 - \prod_{K \neq I} CDF_{I-K}(t) \right] \quad (3)$$

$I$  is an option in the set  $\{2, 3\}$ ,  $J$  is an option in the same set that is not  $I$ , and  $K$  is an option in the set  $\{1, 2, 3\}$  that is not  $I$ . The cumulative distribution functions (CDFs) and probability density functions (PDFs) are those of the standard LBA model (see Terry et al., 2015, also Appendix A). The derivation for Equation 3 may also be found in subsection ‘‘A1. Win-All Derivation’’ of Appendix A.

In the max-next model a decision is made as soon as the difference between the most active and the next most active accumulator exceeds a given threshold. The Win-All model is similar in that a response is made once the winning accumulator has beaten all of its competitors – that is, all relevant accumulators corresponding to pairwise comparisons have exceeded a given threshold. With this rule, the last advantage accumulator to cross its threshold will – on average – represent a contrast between the winner and the next best response option. The Win All ALBA and max-next models are also similar in terms of computational complexity, as for the latter model a full evaluation of the stopping rule must be made at each moment during accumulation. One possible serial algorithm for the max-next stopping rule involves first identifying the accumulator with the highest evidence total, then the one with the second highest, then comparing the difference to a threshold. A possible parallel algorithm could involve evaluating the same set of advantages (in this context differences in momentary evidence totals) as in the ALBA, with a response initiated when an accumulator has both the maximum advantage (and hence must have the maximum evidence total) and a minimum advantage greater than a threshold amount.

The max-next model does not have an easily computed likelihood, so requires the same simulation methods as the LCA to be fit to data in an optimal way, but its computational complexity, like that of the LCA (whose number of lateral inhibitory connections increase with the square of  $n$ ), makes that practically difficult as the number of options increases. In contrast, ALBA does have an easily computed likelihood, which makes it straightforward to fit data from choices among many options, as illustrated below in an application requiring choice among up to 9 options. Before that, we fit data from forced choices among four simultaneously presented options where the max-next model was preferred over independent accumulation (Teodorescu & Usher, 2013).

### Strong versus weak lures

In Experiment 1A reported by Teodorescu and Usher (2013) participants made a forced choice about which of four patches was brightest. The key comparison was between trials that had one relatively attractive incorrect answer and two very unattractive incorrect

answers (from here on, a “difficult trial”) and trials with a set of three relatively unattractive incorrect answers (from here on, an “easy trial”, cf. Teodorescu and Usher, Figure 4). Teodorescu and Usher theorized that, due to the comparatively elevated input of the attractive incorrect answer in the difficult trial, an independent race model will always predict a speed-up for correctly answered difficult trials compared to easy trials, due to statistical facilitation. In contrast, they found correct responses on difficult trials were actually slower than on easy trials.

Eight participants performed between 1,000 and 1,200 trials. Half of these trials constituted the easy condition with luminance values of  $\{.4, .2, .2, .2\}$ , respectively, for the target and three lures. The other half of the trials constituted the difficult condition with brightness values of  $\{.4, .3, .15, .15\}$ . Trials of the easy and difficult condition were randomly mixed within each block. In each condition, the sum of the brightness values is the same, so that normalizing these values by dividing them by the sum preserves the ratios between values, a feature which was used to rule out independent race models with sum-normalized feed-forward input competition. The ALBA is another kind of input-competition model, but with a different architecture and stopping rule.

As described in section “Rethinking stimulus inputs: the two-alternative ALBA”, we assume luminance values are log-transformed to obtain subjective brightness values. Advantage accumulators for each pair are dictated by Equations 1 and 2. Unfortunately, due to a programming error, the data for this experiment only recorded whether the response was correct or incorrect (Teodorescu, personal communication). As a result, in the case of an incorrect response it is unknown which of the incorrect options was chosen. To respect this, we aggregated the model’s log-likelihoods for all three error response options in our fits to the data.

We constrained parameters  $A$ ,  $B$ ,  $t_0$ ,  $v_0$ ,  $w_S$ ,  $w_D$ , and  $s$  to be identical across the two conditions, with a fixed value of  $s = 1$  and the remaining 6 parameters being estimated.<sup>3</sup> Details of the estimation methods are given in subsection “B2. Estimation Details: Strong versus Weak Distractors” in Appendix B. We confirmed the model was identifiable with a parameter-recovery study (for details see subsection “C1. Parameter Recovery Strong versus Weak Distractors” in Appendix C).

Parameter estimates for the Win-All ALBA fit can be found in Table 2. As with our fits to Teodorescu et al. (2016)’s binary choice data, the difference component of the rates had a higher weight than the sum component for all participants, again on average by approximately an order of magnitude. Taking the first participant as a representative example, the mean rates in the easy condition that follow from the median parameter estimates in the Table are 3.1 for the target accumulator and -1.6 for the lure accumulators. Mean rate estimates for the difficult condition involving easy and hard lures bracket these values: for the target relative to the hard and easy lures 1.8 and 4.0, respectively, and for the hard and easy lures -0.1 and -2.6 respectively.

The posterior predictives for the Win-All ALBA are compared against the observed data in Figure 4, showing that the model fits the observed data relatively well. The number

---

<sup>3</sup>We also fit a model that relaxed the assumption of equal rate variability for the easy and difficult condition, estimating it for one and fixing it to  $s = 1$  for the other. Model fit did not qualitatively improve (see subsection “D1. Additional Fits Strong versus Weak Distractors” in Appendix D), so we report the more parsimonious model here.

Table 2

Posterior median parameter values, with a 95% credible intervals for the Win-All ALBA model of Teodorescu and Usher (2013) Experiment 1A data. Rows correspond to participants (Pp), except the top row, which contains parameters of the group-level distributions (Hyper).

Pp	$B$	$A$	$t_0$	$v_0$	$w_S$	$w_D$
Hyper	<b>0.18 (0.01, 0.53)</b>	<b>1.03 (0.21, 1.79)</b>	<b>0.51 (0.11, 0.64)</b>	<b>1.26 (0.43, 1.71)</b>	<b>0.17 (0.01, 0.90)</b>	<b>1.61 (0.45, 3.55)</b>
1	0.05 (0.00, 0.19)	0.87 (0.74, 1.02)	0.66 (0.62, 0.69)	1.33 (0.80, 2.00)	0.23 (0.02, 0.59)	3.38 (2.86, 3.80)
2	0.09 (0.01, 0.32)	1.11 (0.89, 1.35)	0.68 (0.61, 0.72)	1.02 (0.32, 1.70)	0.31 (0.03, 0.78)	3.91 (3.25, 4.62)
3	0.01 (0.00, 2.13)	0.58 (0.15, 0.70)	0.64 (0.27, 0.65)	1.41 (0.91, 10.25)	0.17 (0.00, 3.26)	3.13 (1.32, 3.45)
4	0.11 (0.00, 0.37)	4.07 (3.39, 4.81)	0.48 (0.37, 0.56)	1.28 (0.86, 1.75)	0.09 (0.00, 0.34)	3.69 (3.30, 4.04)
5	0.39 (0.07, 0.75)	1.19 (1.00, 1.38)	0.58 (0.50, 0.65)	1.40 (0.91, 3.42)	0.24 (0.02, 1.49)	4.16 (3.64, 5.48)
6	0.55 (0.23, 1.21)	1.84 (1.52, 2.22)	0.63 (0.50, 0.70)	1.73 (1.24, 2.32)	0.05 (0.00, 0.26)	3.58 (3.10, 4.14)
7	0.35 (0.11, 0.93)	2.34 (1.98, 2.74)	0.60 (0.47, 0.67)	1.57 (1.08, 13.33)	0.21 (0.03, 4.43)	3.95 (1.77, 4.54)
8	0.00 (0.00, 0.07)	0.91 (0.78, 1.07)	0.64 (0.60, 0.66)	0.96 (0.12, 11.39)	0.47 (0.10, 4.15)	4.05 (2.02, 4.41)

of free parameters required to obtain this fit (six) is smaller than the number of free parameters (seven or eight) in the several models that were fit by Teodorescu and Usher (2013). The model misfits accuracy for the difficult condition for some participants, although the aggregate posterior predictive data (right-most column) captures the data at least as well as the best (max-next) model reported by Teodorescu and Usher (2013).

To confirm the shortcomings of a conventional race model with one-to-one accumulator-to-response mapping, we also fit a regular LBA to the data. As only a ‘generic’ error was logged, not which specific error response was given, this LBA included one correct drift rate and one error drift rate for each of the two conditions, along with the standard  $A$ ,  $B$ , and  $t_0$  parameters. This model failed to fit the data satisfactorily; in order to capture the pattern in RTs between the easy and difficult condition it drastically over-predicts error rates in both conditions (see subsection “D1. Additional Fits Strong versus Weak Distractors” in Appendix D). We performed model selection using the Deviance Information Criterion (DIC; Spiegelhalter, Best, Carlin, & van der Linde, 2002), a measure that balances goodness of fit against model complexity. A much smaller DIC for the ALBA (2854) than the LBA (13302) suggests it is a vastly superior model.

In this section, we have demonstrated that the ALBA model can account for the strong versus weak lure data. This result suggests instead of independence, it is the assumption of a one-to-one mapping of accumulators to responses and the associated response rule that is problematic for the class of input-competition models. Next, we turn to another challenging empirical pattern for a multiple-alternative accumulator model: Hick’s Law.

### Hick’s Law

Hick’s Law is a long-standing benchmark result for multiple-alternative decisions (Hick, 1952; Teichner & Krebs, 1974). It states that the mean RT and the logarithm of the number of choice alternatives are approximately linearly related. A well-known problem with independent race models with a one-to-one accumulator to response mapping is that they produce the opposite trend to Hick’s Law, *faster* decisions with more accumulators, because of statistical facilitation (Raab, 1962). Usher, Olami, and McClelland (2002) note that competitive accumulation (i.e., lateral inhibition among accumulators) can produce increasing RT with the number of options (see also Usher & McClelland, 2001), but at least

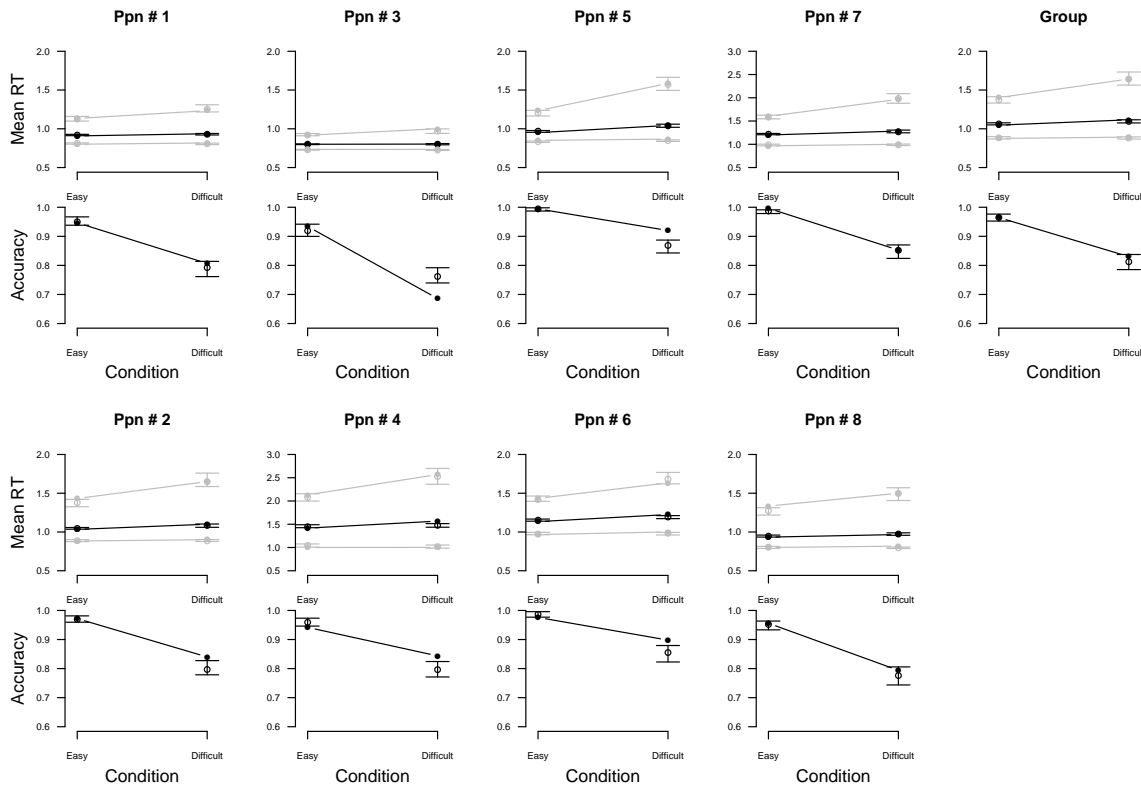


*Figure 4.* Posterior predictive data for fits to the Experiment 1A data of Teodorescu and Usher (2013). RTs for the .5 (black), .1, and .9 (gray) deciles calculated for the easy (top-left) and difficult (top-right) condition, and the proportion of correct responses for the easy (bottom-left) and difficult (bottom-right) condition, both at the individual level (left four columns) and for aggregate data (right column). For all panels, error bars represent posterior predictive data simulated from model fits (the bar extends to the middle 95% of generated summary statistics, with the dot in the middle indicating the median) and lines represent data. See text for details.

in the LCA they found this was not sufficient to quantitatively account for Hick's Law. They then showed that both in the LCA and an independent racing accumulator model, Hick's Law can be accommodated if evidence thresholds are increased with set size in order to compensate for a decrease in accuracy that otherwise occurs as the number of choices increases.

Like the LCA, the Win-All ALBA naturally predicts longer response times as number of options ( $n$ ) increases. This is because at least  $n - 1$  accumulators need to reach threshold before a decision can be triggered. Effectively this means decision time increases as the maximum of a set of random variables (the times for accumulators to each threshold), where the size of that set increases in proportion to  $n$ . Simulations with a range of different random variables indicate the increase is approximately linear to the logarithm of  $n$ . However, the question remains whether the ALBA can quantitatively account for the fine details of RT

and accuracy changes as a function of the number of response options due to this feature of its architecture alone, or whether evidence thresholds or other parameters also need to change with set size.

We took advantage of the tractability of the ALBA to directly fit it to an archival Hick’s Law data set (van Maanen et al., 2012). This approach allows us to go beyond the conventional formulation of Hick’s Law in terms of mean RT, expanding our test of the ALBA to its ability to account for the effects of choice-set-size simultaneously on both accuracy and the full distribution of RT (see also Brown, Marley, Donkin, & Heathcote, 2008a; Hawkins, Brown, Steyvers, & Wagenmakers, 2012a, 2012b).

van Maanen et al. (2012) had participants view displays consisting mostly of randomly moving dots with a subset that move coherently in one direction (Britten, Shadlen, Newsome, & Movshon, 1992). Each trial involved either 3, 5, 7 or 9 directions, with the corresponding number of responses. There were eight blocks of trials, and within each block, trials were pseudo-randomized, such that no more than two consecutive trials had the same number of response options. In the “clustered” condition, which we address here, the angular spacing between adjacent stimulus directions was the same for all set-sizes, and hence the range of stimulus directions increased with set-size, in an attempt to equate perceptual discriminability across set-sizes. All four conditions were administered within all five subjects, and there were 144 trials per condition.

Assume there are  $n$  stimuli, and therefore  $n$  responses matched to stimuli in a 1-to-1 fashion. Let stimulus  $k$ ,  $k \in \{1, \dots, n\}$ , have subjective value  $s_k$ . In the experiment we consider, we assume the stimuli are subjectively equally spaced; that is, there is a subjective stimulus value  $s$  such  $s_i - s_j = (i - j)s$  for all  $i, j \in \{1, \dots, n\}$ . We assume that the subject has a (referent) memory of the subjective value of each stimulus that is presented in the current task. Let  $S_{j|i}$  denote the ‘strength’ of response  $j$  when stimulus  $i$  is presented. Then we assume  $S_{j|i}$  has the form:<sup>4</sup>

$$S_{j|i} = \left( \frac{1}{1 + \frac{|s_j - s_i|}{s}} \right)^\alpha = \left( \frac{1}{1 + |j - i|} \right)^\alpha .$$

with a constant  $\alpha > 0$ . To provide some intuition about this function, consider the condition with five choice options, and a trial in which stimulus 2 is presented. For  $\alpha = 1$ , this leads to the set of input values  $\{0.5, 1, 0.5, 0.33, 0.25\}$ , reflecting the fact that nearby options are more plausible than options further removed. For  $\alpha = \infty$ , this leads to the set of input values  $\{0, 1, 0, 0, 0\}$ , reflecting no difference in the input values for competitors (i.e., no effect of proximity). Calculation of drift rates for each advantage accumulator followed a slightly modified version of Equations 1 and 2 to account for the fact that inputs depend on the angular distance from the correct response:

$$v_{j-k|i} = v_0 + w_S(S_{j|i} + S_{k|i}) + w_D(S_{j|i} - S_{k|i}) \quad (4)$$

$$v_{k-j|i} = v_0 + w_S(S_{j|i} + S_{k|i}) + w_D(S_{k|i} - S_{j|i}) \quad (5)$$

<sup>4</sup>The presented form is for stimuli that are subjectively equally spaced and, as we see later, does not fit certain data for stimuli at, or near, the ends of the range of presented stimuli well. A complete theory, building on the current assumptions, might include a *rehearsal component*, similar to that in SAMBA (Brown et al., 2008a).

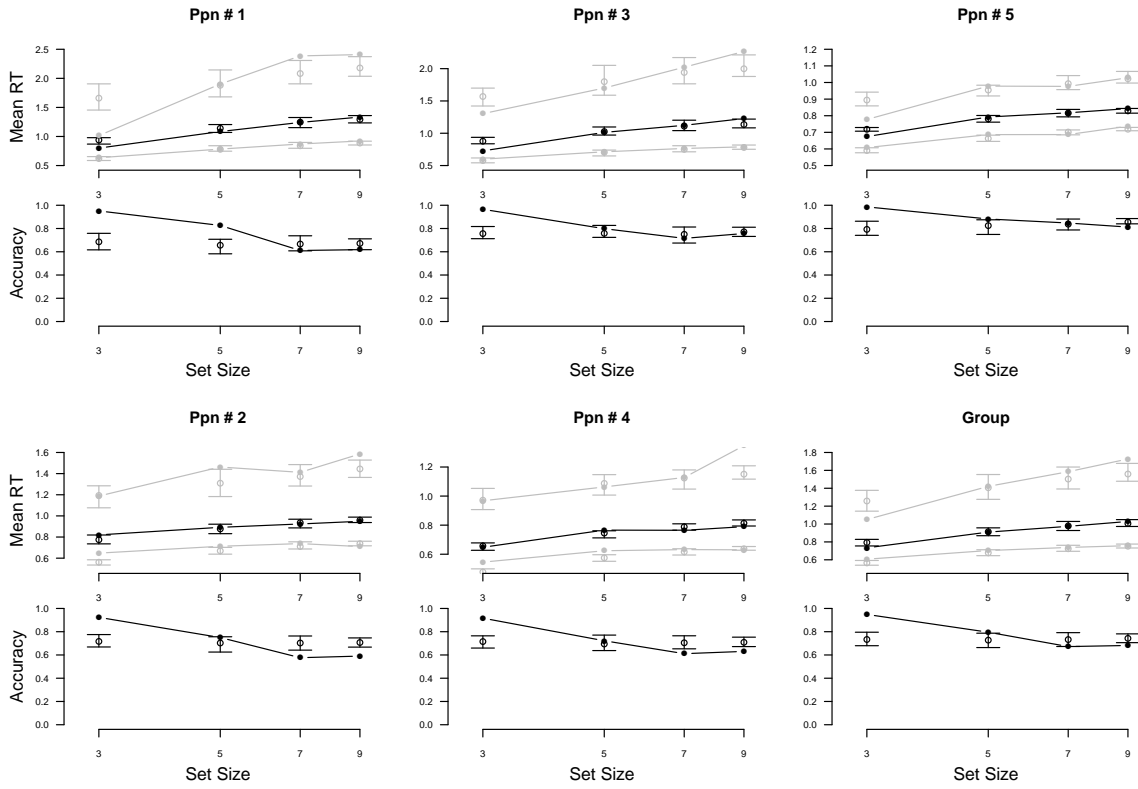


Figure 5. Posterior predictive data for the ALBA-1 fit to the van Maanen data. RTs for the .5 (black), .1, and .9 (gray) deciles (top) and the proportion of correct responses (bottom) as a function of set-size ( $N$ ) on a logarithmic scale. Posterior predictives are presented at the individual level and for aggregate data (bottom-right panel). For all panels, box-and-whiskers represent posterior predictive data (the box contains 95% of the simulated data, with a bar across the middle indicating the median, and whiskers extend to the data extremes) and lines represent data. See text for details.

Details of model fitting can be found in the subsection “B3. Estimation Details: Hick’s Law” in Appendix B. We confirmed the model was identifiable with a parameter-recovery study (for details see subsection “C2. Parameter Recovery Hick’s Law” in Appendix C). In order to see if the Win-All ALBA naturally produces Hick’s Law we fit a model that constrained all parameters to be equal across set-size conditions (i.e.,  $B$ ,  $A$ ,  $t_0$ ,  $v_0$ ,  $w_S$ ,  $w_D$ , and  $\alpha$ ), with a fixed value of  $s = 1$  (ALBA-1). Estimated parameters for the resulting model are given in Table 3. The pattern of weight parameters follows that found in earlier fits with the difference weight more than an order of magnitude greater than the sum weight. Although estimates of  $\alpha$  are relatively small, mean rates change monotonically with the distance between inputs. For example, based on the median posterior parameter estimates for the first participant, mean rates for the accumulator associated with the advantage of the correct choice over options 1, 2, and 3 spaces removed are 1.1, 1.7, and 2.1, respectively. Similarly, for the advantage accumulator associated with choice options 1, 2, and 3 spaces



Table 3

*Estimated parameters of the ALBA-1 model for the van Maanen data set. Displayed are the median parameter values, with a 95% credible interval of the posterior presented in parentheses. Rows correspond to participants (Pp), except the top row, which contains parameters of the group-level distributions (Hyper).*

Pp	$B$	$A$	$t_0$	$v_0$	$w_S$	$w_D$	$\alpha$
<b>Hyper</b>	<b>0.11 (0.01, 0.32)</b>	<b>1.18 (0.94, 1.45)</b>	<b>0.34 (0.19, 0.41)</b>	<b>0.20 (0.01, 0.80)</b>	<b>0.34 (0.04, 0.73)</b>	<b>10.00 (4.58, 15.17)</b>	<b>0.16 (0.07, 0.48)</b>
1	0.11 (0.01, 0.32)	1.22 (1.02, 1.51)	0.33 (0.25, 0.39)	0.13 (0.01, 0.43)	0.13 (0.01, 0.34)	10.21 (3.95, 19.08)	0.14 (0.08, 0.40)
2	0.05 (0.00, 0.17)	1.14 (0.94, 1.34)	0.37 (0.32, 0.42)	0.32 (0.02, 0.86)	0.27 (0.02, 0.51)	16.56 (10.64, 26.53)	0.09 (0.05, 0.14)
3	0.14 (0.03, 0.38)	1.25 (1.03, 1.56)	0.30 (0.20, 0.36)	0.12 (0.01, 0.42)	0.11 (0.00, 0.36)	12.17 (4.03, 21.38)	0.15 (0.09, 0.44)
4	0.05 (0.00, 0.17)	1.03 (0.82, 1.22)	0.33 (0.27, 0.37)	0.28 (0.02, 0.99)	0.42 (0.06, 0.65)	14.88 (9.89, 23.64)	0.09 (0.06, 0.14)
5	0.19 (0.06, 0.40)	1.19 (1.02, 1.44)	0.43 (0.37, 0.46)	0.20 (0.01, 1.38)	1.12 (0.27, 1.42)	4.49 (3.02, 15.19)	0.38 (0.12, 0.58)

removed from the correct choice mean rates were -0.9, -1.5, and -1.9 respectively. Estimates of  $A$  were quite large, indicating strong effects of factors like response biases due to carry-over effects from previous responses (Heathcote, Suraev, Curley, Gong, & Love, 2015). In comparison  $B$  estimates were small, although they were in most cases clearly greater than zero, indicating that participants exercised a small degree of response caution.

As shown in Figure 5, the model fit the median RT data well, consistent with the ALBA architecture accommodating the logarithmically increasing effect of set-size. It also fit effects on fast RTs, but did not fit the increase in error rates with set size and RTs in the slow tail of the distributions for higher set sizes. Given the misfit we explored models that allowed selected parameters to change with set size  $n$ . These analyses demonstrate how the ALBA's easily computed likelihood makes it practical to fit and evaluate a range of alternative model parameterizations. DIC values for all models can be found in Table 4. The table also reports the two components of DIC, one of which quantifies the model misfit, and the other that determines the penalty for model complexity.

Following Usher et al. (2002), we first examined a model that allowed thresholds to vary across set-size conditions. Varying threshold with set size could occur because set-size was manipulated between blocks of trials so participants could implement a trade off between speed and accuracy (model ALBA-4B). Although there were small improvements in both DIC and the account of accuracy effects, there was still clear misfit (see Appendix D, Figure D3).

Given that the observed misfit pertained to RT distribution and accuracy, it is likely to be explicable by a model that allows parameters determining the level of trial-to-trial variability to change with set size. We first considered start-point noise ( $A$ ). Start-point noise is usually attributed to factors like response biases due to carry-over effects from previous responses (Heathcote et al., 2015) and so could plausibly vary with the number of responses. We allowed a different value of  $A$  for every set-size (ALBA-4A), with all other parameters constrained to be equal across set-size conditions. However, although DIC and the fit were again slightly improved, substantial misfit was still evident (see Appendix D, Figure D4).

We next considered rate variability ( $s$ ), and inspired by the work of Ratcliff et al. (2018), we fit a model that allowed it to change linearly with the mean rate and set-size (model ALBA- $\beta$ ). This was achieved by estimating one additional free (slope) parameter,  $\beta$ , where  $s_n = 1 + \beta \times (n - 3) \times v$ . Note that this fixes  $s = 1$  for the smallest set-size

Table 4

*DIC summed over participants for ALBA fits to the van Maanen et al. (2012) data. Parameter(s) varying with set-size, ALBA-1: None, ALBA-4B: B, ALBA-4A: A, ALBA-4BA: both B and A, ALBA- $\beta$ : s, ALBA- $\beta$ 4B: both s and B. # Pars = number of free parameters per participant for all four conditions; Misfit = -2 times the likelihood of the median parameter estimate; Complexity = -4 times the median likelihood of the overall model + 4 times the likelihood of the median parameter estimate; DIC = Misfit + Complexity*

Model	# Pars	Misfit	Complexity	DIC
ALBA-1	7	6439	36	6475
ALBA-4B	10	6399	-15	6384
ALBA-4A	10	6303	56	6359
ALBA-4BA	13	6020	66	6085
ALBA- $\beta$	8	6045	-8	6037
ALBA- $\beta$ 4B	11	5925	17	5943

( $N=3$ ), which makes the model identifiable. Note also that we bounded the value of  $s_n$  below by 0.01 to enforce the necessary non-negativity of a standard deviation. Again all other parameters were constrained to be equal across set-size conditions. Despite requiring the estimation of only one extra parameter, there was a very substantial reduction in misfit and improvement in DIC. As shown in Figure 6, this model produced a good fit to almost all aspects of the data, including the decrease in accuracy with increasing set-size, with only accuracy for set-size 3 being underestimated.

Estimated parameters for the ALBA- $\beta$  model are given in Table 5. Estimates of  $\beta$  were small and positive for all participants, so  $s$  increased with the mean rate. Mean rates were more extreme than those for the baseline (ALBA-1) model. For example, based on the median parameter estimates for the first participant, mean rates were 4.8, 6.5, and 7.8 for the correct choice over options 1, 2, and 3 spaces removed, respectively, and -1.2, -3.0, and -4.3 for choice options 1, 2, and 3 spaces removed relative to the correct choice. This occurred because  $s$  estimates were greater than  $s = 1$  for larger set sizes, which leads to more errors. For set-size 5, for example,  $s$  values associated with the correct choice over options 1, 2, and 3 spaces removed were 2.3, 2.7, and 3.0, respectively, although this was partially compensated for by decreased variability for choice options 1, 2, and 3 spaces removed from the correct choice, with values of 0.7, 0.2, and 0.01, respectively. The other parameter values shared with the ALBA-1 model were similar, except that  $\alpha$  was larger, producing a shallower decrease in rates with distance from the stimulus direction, and  $B$  was close to zero, indicating that participants exercised minimal response caution.

Finally, we examined two models that allowed threshold ( $B$ ) to vary with set size in addition to parameters  $A$  and  $s$  respectively. For the case where  $A$  varies with set size (model ALBA-4BA) there was a very large improvement in DIC, although this was still not sufficient to be selected over the much simpler ALBA- $\beta$  model. ALBA-4BA under-predicts accuracy for the smallest set size and over-predicts accuracy for the two largest set-sizes (Appendix D, Figure D5).

The case where  $B$  and  $s$  vary with set size (model ALBA- $\beta$ 4B) produced the lowest

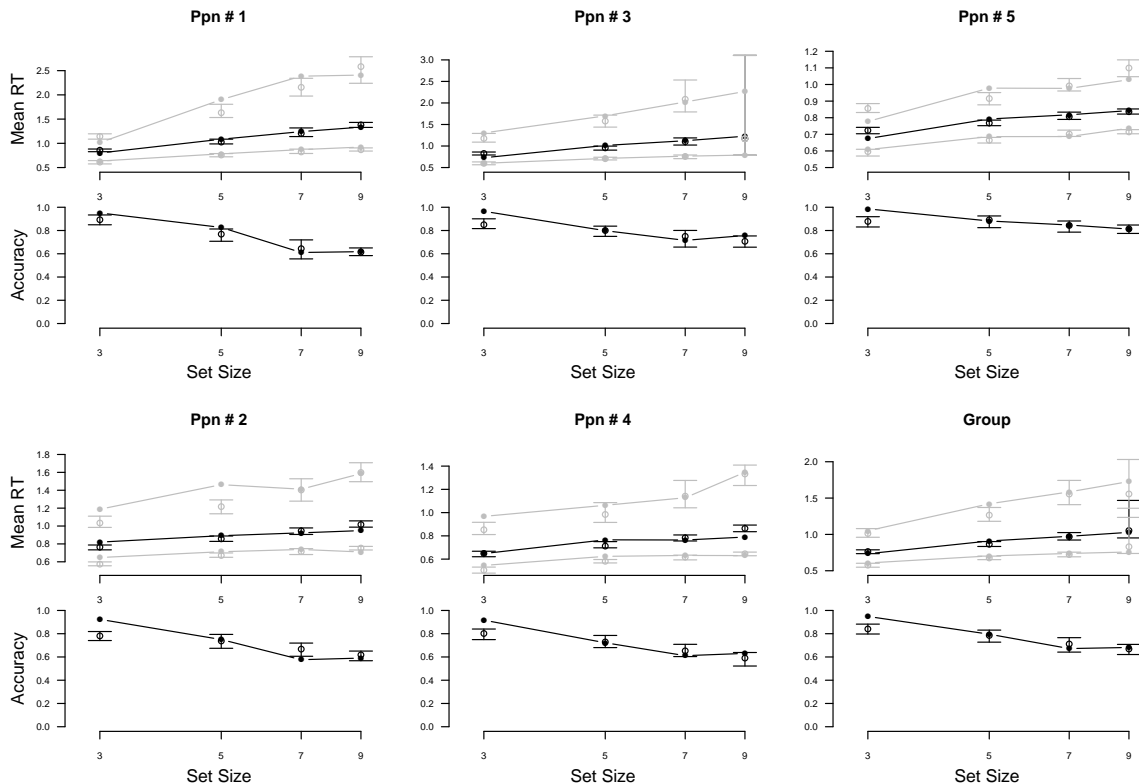


Figure 6. Posterior predictive data for the ALBA- $\beta$  fit to the van Maanen data. RTs for the .5 (black), .1, and .9 (gray) deciles (top) and the proportion of correct responses (bottom) as a function of set-size ( $N$ ) on a logarithmic scale. Posterior predictives are presented at the individual level and for aggregate data (bottom-right panel). For all panels, box-and-whiskers represent posterior predictive data (the box contains 95% of the simulated data, with a bar across the middle indicating the median, and whiskers extend to the data extremes) and lines represent data. See text for details.

DIC of any model in Table 4 but the improvement compared to the ALBA- $\beta$  model was modest. Figure 7 shows that accuracy for set-size 3 is now captured slightly better than the ALBA- $\beta$  model, but is still somewhat under-predicted by the model. Estimated parameters for the ALBA- $\beta$ 4B model are given in Table 6. Most parameters shared with the ALBA- $\beta$  follow a similar pattern. The  $B$  parameters for the ALBA- $\beta$ 4B generally decrease as set size increases, starting at values similar to the ALBA-1 model for smaller set sizes with the values for  $n = 9$  being similar to the single estimate for the ALBA- $\beta$  at close to zero, indicating a very low level of response caution.

As a baseline model for comparison, we fit a standard LBA model to the data, in which we left  $A$ ,  $B$ ,  $v_c$  (corresponding to mean drift rate matching the correct direction), and  $v_e$  (corresponding to mean drift rate not matching the correct direction) free to vary with set size, but constrained  $t_0$  to be equal across set size. The latter model with 17 free parameters failed to fit the data satisfactorily, because it overestimated the increase in error

Table 5

*Estimated parameters of the ALBA- $\beta$  model for the van Maanen data set. Displayed are the median parameter values, with a 95% credible interval of the posterior presented in parentheses. Rows correspond to participants (Pp), except the top row, which contains parameters of the group-level distributions (Hyper).*

Pp	$B$	$A$	$t_0$	$v_0$	$w_S$	$w_D$	$\alpha$	$\beta$
<b>Hyper</b>	<b>0.01 (0.00, 0.05)</b>	<b>1.76 (0.84, 2.48)</b>	<b>0.41 (0.28, 0.46)</b>	<b>1.21 (0.35, 1.80)</b>	<b>0.20 (0.01, 0.61)</b>	<b>9.08 (4.67, 13.37)</b>	<b>0.32 (0.10, 1.00)</b>	<b>0.07 (0.01, 0.13)</b>
1	0.01 (0.00, 0.04)	2.61 (2.05, 3.31)	0.42 (0.37, 0.46)	1.87 (1.18, 2.48)	0.08 (0.00, 0.31)	3.30 (2.79, 5.73)	1.32 (0.41, 1.70)	0.13 (0.07, 0.17)
2	0.01 (0.00, 0.05)	1.48 (1.23, 1.80)	0.42 (0.39, 0.44)	1.19 (0.43, 1.58)	0.12 (0.01, 0.51)	14.49 (7.44, 25.39)	0.13 (0.07, 0.26)	0.05 (0.04, 0.06)
3	0.01 (0.00, 0.07)	1.79 (1.46, 2.21)	0.42 (0.38, 0.45)	0.92 (0.17, 1.40)	0.15 (0.01, 0.56)	11.60 (4.16, 20.97)	0.21 (0.11, 0.68)	0.10 (0.07, 0.12)
4	0.01 (0.00, 0.03)	1.21 (1.02, 1.45)	0.39 (0.37, 0.41)	1.28 (0.50, 1.73)	0.16 (0.01, 0.57)	13.30 (8.01, 24.51)	0.15 (0.08, 0.26)	0.06 (0.05, 0.08)
5	0.01 (0.00, 0.10)	1.80 (1.43, 2.28)	0.49 (0.46, 0.51)	1.78 (0.45, 3.03)	0.57 (0.03, 1.38)	10.80 (6.12, 20.18)	0.30 (0.16, 0.56)	0.03 (0.02, 0.04)

Table 6

*Estimated parameters of the ALBA- $\beta_4B$  model for the van Maanen data set. Displayed are the median parameter values, with a 95% credible interval of the posterior presented in parentheses. Rows correspond to participants (Pp), except the top row, which contains parameters of the group-level distributions (Hyper).*

Pp	$B_3$	$B_5$	$B_7$	$B_9$	$A$	$t_0$
<b>Hyper</b>	<b>0.12 (0.01, 0.35)</b>	<b>0.16 (0.03, 0.31)</b>	<b>0.05 (0.00, 0.14)</b>	<b>0.01 (0.00, 0.07)</b>	<b>1.81 (1.20, 2.41)</b>	<b>0.39 (0.22, 0.45)</b>
1	0.06 (0.00, 0.19)	0.21 (0.12, 0.34)	0.07 (0.01, 0.17)	0.01 (0.00, 0.03)	2.40 (1.80, 3.09)	0.41 (0.35, 0.45)
2	0.30 (0.21, 0.41)	0.19 (0.12, 0.28)	0.06 (0.01, 0.12)	0.01 (0.00, 0.03)	1.58 (1.30, 1.90)	0.39 (0.35, 0.42)
3	0.09 (0.01, 0.18)	0.11 (0.02, 0.18)	0.03 (0.00, 0.09)	0.02 (0.00, 0.11)	1.83 (1.52, 2.22)	0.39 (0.36, 0.43)
4	0.18 (0.10, 0.28)	0.13 (0.06, 0.21)	0.04 (0.00, 0.10)	0.01 (0.00, 0.04)	1.43 (1.19, 1.77)	0.35 (0.32, 0.37)
5	0.03 (0.00, 0.11)	0.19 (0.11, 0.31)	0.06 (0.01, 0.17)	0.02 (0.00, 0.12)	1.81 (1.49, 2.34)	0.48 (0.45, 0.50)

Pp	$v_0$	$w_S$	$w_D$	$\alpha$	$\beta$
<b>Hyper</b>	<b>1.10 (0.31, 1.73)</b>	<b>0.35 (0.03, 0.77)</b>	<b>8.19 (4.57, 11.88)</b>	<b>0.37 (0.14, 1)</b>	<b>0.07 (0.01, 0.12)</b>
1	1.73 (1.16, 2.28)	0.07 (0.00, 0.34)	3.33 (2.69, 6.20)	1.19 (0.37, 1.61)	0.12 (0.07, 0.15)
2	1.10 (0.18, 1.73)	0.31 (0.02, 0.82)	11.27 (7.06, 17.63)	0.17 (0.11, 0.30)	0.06 (0.05, 0.07)
3	0.91 (0.13, 1.43)	0.21 (0.01, 0.64)	9.63 (5.17, 18.86)	0.26 (0.12, 0.55)	0.10 (0.08, 0.12)
4	1.22 (0.23, 1.95)	0.39 (0.03, 0.97)	12.10 (7.42, 20.98)	0.17 (0.10, 0.30)	0.06 (0.05, 0.08)
5	1.30 (0.23, 2.93)	1.06 (0.19, 1.79)	8.19 (5.08, 13.01)	0.41 (0.25, 0.65)	0.03 (0.03, 0.04)

rate for increasing set sizes (for details, see Appendix D). Fits presented in van Maanen et al. (2012) are based on even larger numbers of free parameters.

In summary, these analyses clearly show that the Win-All ALBA naturally predicts Hicks Law in terms of the central tendency of RT, and is able to capture most fine-grained effects of set size on accuracy and RT distribution when some of its parameters are allowed to change with set size. In the data set examined here (van Maanen et al., 2012) there was strong support for a parsimonious account in terms of a linear effect of set size on a proportional relationship between the mean and standard deviation of variability in rates, and some evidence for a decrease in response caution as set size increased. Whether such effects apply to other instances of Hick’s Law remains to be seen. The remaining misfit, under-prediction of accuracy for a set size of 3, may not have been due to the Win-All ALBA itself but instead because of our specification of the way mean rates change as a function of distance from the correct response. Although the function we specified is flexible, it does not take account of “edge effects” – improved discriminability for stimuli at the extremes of the stimulus set – which are known to be prevalent in absolute identification tasks, such as the present one, that require classification of stimuli along a single dimension (Brown, Marley, Donkin, & Heathcote, 2008b). For  $n = 3$  the majority of the stimuli are at the

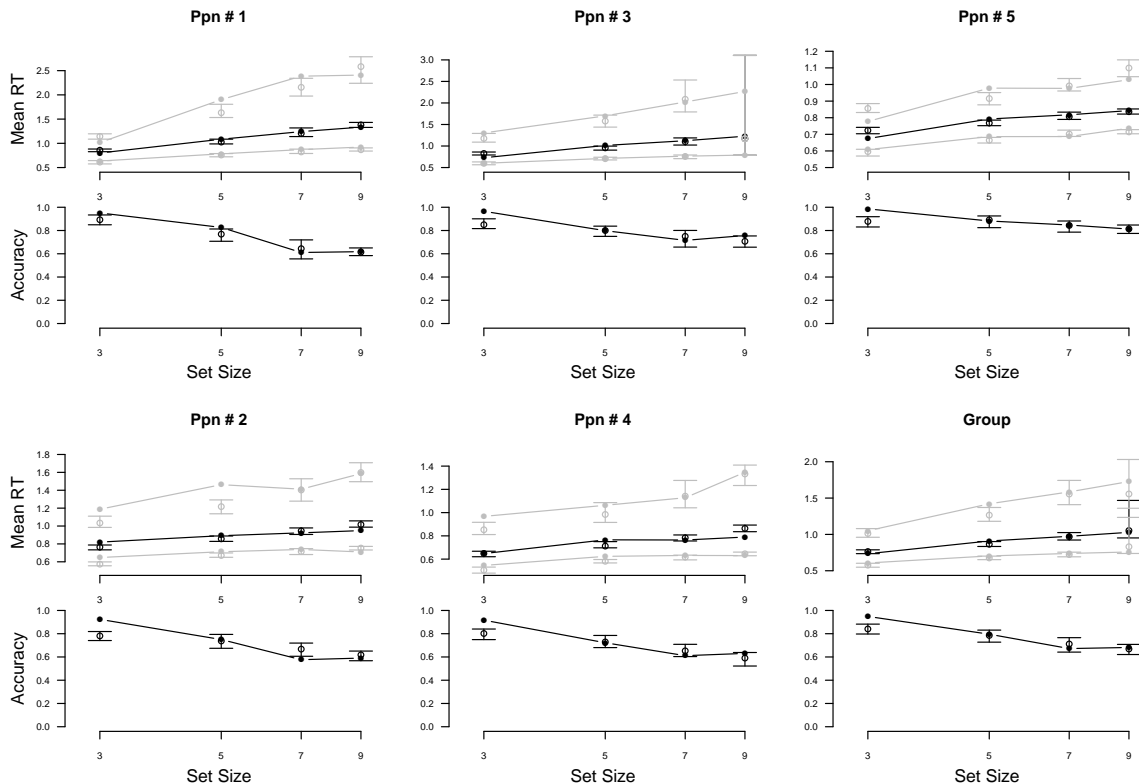


Figure 7. Posterior predictive data for the ALBA- $\beta$ 4B fit to the van Maanen data. RTs for the .5 (black), .1, and .9 (gray) deciles (top) and the proportion of correct responses (bottom) as a function of set-size ( $N$ ) on a logarithmic scale. Posterior predictives are presented at the individual level and for aggregate data (bottom-right panel). For all panels, box-and-whiskers represent posterior predictive data (the box contains 95% of the simulated data, with a bar across the middle indicating the median, and whiskers extend to the data extremes) and lines represent data. See text for details.

edges, whereas this proportion drops off rapidly as  $n$  increases, consistent with a pronounced under-prediction of accuracy for  $n = 3$ .

## Discussion

In this paper we proposed a dynamic theory of multiple choice decisions in terms of *advantages*, directed pairwise comparisons among the subjective values of response alternatives. We instantiated this theory through a linear scheme for mapping subjective values to the inputs for linear evidence accumulation processes that race independently to determine a choice. The linear and independent nature of this “Advantage LBA” (ALBA) model makes it sufficiently mathematically tractable to support an easily computed likelihood. We exploited this likelihood to explore the ability of the model to provide a comprehensive fit to both choice probabilities and the full distribution of RT. We addressed tasks requiring either identification or forced choice among sets of responses ranging in size from two

to nine, with a focus on phenomena that have been claimed to rule out independent race models. Contrary to these claims, the ALBA provided a good account of these data in a parsimonious and parametrically plausible and coherent manner.

We first focused on a task requiring two-alternative forced choices based on brightness (Teodorescu et al., 2016, Experiment 1). We exploited the known luminance values and research supporting a logarithmic mapping to subjective brightness values (Fechner et al., 1966) to test a linear mapping to the rate of evidence accumulation in terms of three estimated parameters, an intercept and weights on the sum of and difference between the subjective brightness values for the two options being compared by each advantage accumulator. We described this as an “advantage-input” coding scheme because it is the difference component that determines whether responses are accurate. Consistent with this nomenclature, the difference weight was estimated as an order of magnitude greater than the sum weight. This finding was replicated in our two subsequent applications of the ALBA, for choices among more than two brightness values and movement directions in forced choice and identification respectively, bolstering the plausibility of the advantage-input coding scheme. In all cases the sum weight, although smaller, was non-negligible, consistent with Teodorescu et al.’s thesis that forced choice has both absolute and relative components.

Although we focused on cases in which objective stimulus values are known and a mapping assumed that produces corresponding subjective values for each stimulus, the advantage-input coding scheme also enables subjective values to be directly estimated, at least when there are sufficiently many stimuli. In binary choice, for example, with only two stimuli the corresponding two subjective values cannot be identified because a total of 5 parameters must be estimated (i.e., the two subjective values and three advantage-input parameters) in order to specify four rates (i.e., inputs for each of the two accumulator for each stimulus). However, with three stimuli identification is possible because 6 estimated parameters are sufficient to estimate the six required rates. As the number of stimuli ( $S$ ) increases estimates become increasingly constrained as only  $S+3$  parameters are required to calculate  $2S$  rates. Thus, our approach provides a method to estimate a scaling of subjective values for a set of three or more stimuli based on binary responses that, for the first time to our knowledge, takes account of RT as well as choices. This approach can be applied when objective values are unknown (e.g., for items in a recognition memory experiment) and when they are known to infer an unknown mapping to subjective values.

The same logic applies to choices among more than two options, which may offer efficiencies above standard methods of obtaining a scaling based on testing all possible binary comparisons among a set of stimuli, as all such binary comparisons are assumed to occur as part of the ALBA architecture. Clearly further work is needed to determine the best designs to realize these potential efficiencies. Our applications here focused on cases like brightness judgments where a unidimensional scaling of subjective values is likely to apply. However, our approach could be applied more broadly to cases where multidimensional scalings might be required, such as in multiattribute choice. In this case subjective coordinates would be estimated and differences taken according to an assumed distance metric (e.g., Euclidean or City Block), and goodness of fit used to adjudicate among potential choices of dimensionality and metric.

In cases where simple scalability fails, such as the multiattribute choice context effects studied by Trueblood et al. (2014), a potential approach is an architecture in which there is

a separate ALBA for each attribute, so each attribute is treated like a separate stimulus, and an appropriate stopping rule applied to combine the outputs of each ALBA. In Appendix E we investigated a Win-All type stopping rule, choosing the option whose entire set of advantages (for both attributes) finishes first. We obtained the attraction effect (Huber, Payne, & Puto, 1982), where an indifferent forced binary choice is tipped towards one option in a trinary choice by adding a stimulus that is equal on one attribute and slightly inferior on the other to the now favored stimulus. We also obtained the compromise effect (Simonson, 1989), where the added stimulus is clearly dominated on one attribute and dominates on the other attribute relative to the new favored stimulus, but less so than the now disfavored stimulus. We are certainly not claiming that this version of the Win-All ALBA provides the same sort of comprehensive account of context effects as models like Trueblood et al.’s MLBA, but merely offer this finding as a demonstration that the ALBA is not necessarily incompatible with, and offers a potential alternative approach to, phenomena that violate simple scalability.

We next focused on a four-alternative forced-choice task, again requiring selection of the brightest stimulus (Teodorescu & Usher, 2013), so we used the same method of determining rates from objective stimulus values. With  $n = 4$  possible responses there are  $n(n - 1) = 12$  advantage accumulators, with each response being associated with a set of  $n - 1$  advantages. We showed that a Win-All decision rule was able to accommodate the “near-competitor” effect, whereby decisions are slower and less accurate when a lure stimulus is close in value to the correct stimulus. This occurs under the Win-All rule because decision time is determined by the *slowest* member of the winner’s set of  $n - 1$  advantages, which for an accurate response will typically correspond to the contrast between the correct stimulus and the near competitor. As the later contrast has, by definition, a slow rate (due to a small difference) the near-competitor effect arises.

Our final application was to an identification task that varied the number of potential responses between  $n = 3$  and  $n = 9$  (van Maanen et al., 2012), with a focus on Hick’s Law, a linear increase in mean RT with the logarithm of  $n$ . Hick’s Law is problematic for independent race models with a one-to-one mapping between stimuli and accumulators, because decision time corresponds to the *minimum* of the  $n$  accumulator completion times, which, all other things being equal, decreases with  $n$ . For the Win-All ALBA the same logic about a minimum time applies, but to the counters that require all of their  $n - 1$  accumulators to complete before they complete. Hence, all other things are not equal, as the completion time of a counter depends on the *maximum* completion time over its  $n - 1$  accumulators, which increases with  $n$ . We showed that Hick’s Law naturally emerges from this “minimum-of-maxima” setup.

The Win-All stopping rule was a key enabler in successfully extending the ALBA to tasks with more than two choices. However, it is only one of a variety of potential stopping rules. In the appendix, we detail two alternative stopping rules. The Lose-All rule assumes that the decision maker responds as soon as all but one of the response options have been beaten by every other contrasting alternative. The Lose-One rule assumes that the decision maker responds as soon as all but one of the response options have been beaten by at least one contrasting alternative. We focused on the Win-All rule because of its conceptual similarity to max-next models, because of the relatively transparent way in which it explains the near-competitor effects and Hick’s Law, and because it provided the best fit to the data

we examined. However, we do not believe it would be prudent to conclude that the later finding will always hold, that the same stopping rule necessarily applies in all situations, or indeed that the three we considered are the only possibilities. That said, at present we recommend the Win-All rule as the default choice for applications of the ALBA.

Our further analysis of van Maanen et al.'s data (2012) showcased the power afforded by the ALBA's easily computed likelihood in terms of our ability to relatively easily fit and evaluate a range of alternative model parameterizations despite the computational complexity associated with  $n = 9$  choices, and hence  $n(n - 1) = 72$  accumulators. We were able to explore six models with Bayesian methods that enabled us to thoroughly evaluate and compare them. This also demonstrated the application of a flexible functional method for determining subjective values from objective stimulus values. We did not intend either the proposed mapping or the model exploration to be definitive, but rather as illustrative of the potential for future applications of the ALBA. Even so, we were able to show that the ALBA was able to fit fine-grained detail in a complex data set.

The ALBA shares with the LCA and max-next models a high degree of computational complexity that either scales with the square of the number of possible responses or involves some serial components. In the LCA this occurs because, although there are only  $n$  accumulators,  $n^2$  lateral inhibitory connections are required. For the max-next model this occurs either because several serial operations are required at each moment during accumulation or because a parallel version requires the same order of advantage comparisons as the ALBA. A common element here is the requirement to base decisions on some sort of pairwise comparison among potential responses, which naturally leads to a rapid increase in computational cost with  $n$ . Although ways to avoid this have been proposed, such as normalizing inputs, it has been argued that this approach is inadequate (Teodorescu & Usher, 2013), so high computational cost may be unavoidable. The ALBA expresses this cost in terms of a complex architecture, but we would argue that it is no more costly than other proposals with a similar explanatory reach, and quite plausible given the brain's massively parallel architecture.

In conclusion, this paper presents a new framework for modeling multialternative speeded choice response data. This framework is based on racing accumulators corresponding to binary advantages of choice options. The result is a tractable accumulator model that can account for a number of benchmark data sets with explicit expressions for likelihood functions that allow direct fitting to data and psychologically interpretable parameters.

### Acknowledgements

This research was supported by Australian Research Council grants to DvR, SDB, and AH (DE140101181, FT120100244, DP12102907, DP160101891 and DP110100234) and a Natural Science and Engineering Research Council Discovery Grant (8124-98) to AAJM. The work was carried out, in part, while Marley was a Distinguished Professor (part-time) at the Institute for Choice, University of South Australia Business School.



Appendix A  
ALBA Stopping Rules

All stopping rules for the ALBA require access to an analytical expression for the probability density function and cumulative density function of a single accumulator. As shown in Terry et al. (2015), the cumulative distribution function (CDF) for the random variable associated with the decision time ( $t \geq 0$ ) of a single accumulator is given by:

$$CDF(t) = 1 + \left( \frac{tZ(t) - b}{A} \right) G\left(\frac{b}{t}\right) + \left( \frac{b - A - tZ(t)}{A} \right) G\left(\frac{b - A}{t}\right) \quad (6)$$

with

$$Z(t) = \frac{1}{G\left(\frac{b}{t}\right) - G\left(\frac{b-A}{t}\right)} \int_{\frac{b-A}{t}}^{\frac{b}{t}} ug(u) du \quad (7)$$

Here,  $G$  and  $g$  represent the cumulative distribution function and probability density function for the distribution of drift rates, respectively. The PDF for finishing times of a single accumulator is obtained by differentiation of (6) with respect to  $t$ . Assuming  $Z(t)$  is differentiable for all  $t > 0$ , and denoting its derivative by  $Z'(t)$ , we get

$$PDF(t) = \left( \frac{Z(t) + tZ'(t)}{A} \right) \left[ G\left(\frac{b}{t}\right) - G\left(\frac{b-A}{t}\right) \right] + \left( \frac{tZ(t) - b}{A} \right) g\left(\frac{b}{t}\right) \left( \frac{b - A - tZ(t)}{A} \right) g\left(\frac{b - A}{t}\right) \quad (8)$$

Note that Equations 6 and 8 only involve the expressions for the PDF and CDF of the drift rate distribution ( $g$  and  $G$  respectively). This results in expressions for the PDF and CDF for a single accumulator that are analogous to those presented as Equations (1) and (2) of Brown and Heathcote (2008).

### A1. Win-All Derivation

In this section, we unpack the equations for the Win-All version of the ALBA model, (3) for a decision trial with three response options (i.e., 1, 2, and 3). It can be written out as:

$$p_1(t) = PDF_{1-2}(t) \times CDF_{1-3}(t) \times \prod_{I \neq A} \left[ 1 - \prod_{K \neq I} CDF_{I-K}(t) \right] + \quad (9)$$

$$PDF_{1-3}(t) \times CDF_{1-2}(t) \times \prod_{I \neq A} \left[ 1 - \prod_{K \neq I} CDF_{I-K}(t) \right]$$

where  $I$  is an option in the set  $\{2, 3\}$  and  $K$  is an option in the set  $\{1, 2, 3\}$  that is not  $I$ . The first line represents the scenario where accumulator 1 – 2 is the terminating accumulator that prompts the response ( $PDF_{1-2}(t)$ ), accumulator 1 – 3 had finished before ( $CDF_{1-3}(t)$ ), and at least one accumulator out of each of the sets  $\{2 - 1, 2 - 3\}$ , and  $\{3 - 1, 3 - 2\}$  had not yet finished ( $\prod_{I \neq 1} [1 - \prod_{K \neq I} CDF_{I-K}(t)]$ ).

Similarly, the second line represents the scenario where accumulator 1 – 3 is the terminating accumulator that prompts the response ( $PDF_{1-3}(t)$ ), accumulator had finished

before ( $CDF_{1-2}(t)$ ), and at least one accumulator out of each of the sets  $\{2-1, 2-3\}$ , and  $\{3-1, 3-2\}$  had not yet finished ( $\prod_{I \neq 1} [1 - \prod_{K \neq I} CDF_{I-K}(t)]$ ).

The PDF for response 1 is completed by summing the expressions on both of these lines.

## A2. Lose-All Stopping Rule

The Lose-All model assumes that the decision maker responds as soon as all but one of the response options have been beaten by every other contrasting alternative; thus, the Lose-All model is a “last man standing” algorithm, and the conceptual inverse of the Win-All model. For example, the decision maker chooses 1 from three response options (i.e., 1, 2, and 3) if and only if

1. All of the accumulators in each of the sets  $\{1-2, 3-2\}$ , and  $\{1-3, 2-3\}$  have reached their threshold, and:
2. At least one of the accumulators in the set  $\{2-1, 3-1\}$  has *not* reached its threshold.

Specifically, response option 1 is the sole remaining option that has not yet been beaten by *every* competitor. This rule could be instantiated by linking each response with a counter having six inputs (e.g., all but 1-2, and 1-3 for a 1 response) and requiring six counts to trigger its response.

Again, accumulator termination sequences can arise that look somewhat contradictory. For example, consider the following sequence of accumulators reaching threshold: all of the accumulators in  $\{1-2, 1-3\}$ , followed by accumulators  $\{2-1, 3-1\}$ , and  $\{2-3\}$ . Then response 2 is made, despite the fact that 1 started out beating every competitor. Again, with sensible drift rates, this set of events is exceedingly unlikely.

The probability density function for the distribution of responses 1 at time  $t$  is given by

$$p_1(t) = \sum_{I \neq 1} \left[ \sum_{J \neq I} \left( PDF_{J-I}(t) \times \prod_{K \neq I, J} CDF_{K-I}(t) \times \prod_{L \neq I, 1} \prod_{M \neq L} CDF_{M-L}(t) \right) \right] \times \left( 1 - \prod_{I \neq 1} CDF_{I-1}(t) \right) \quad (10)$$

$I$  is an option in the set  $\{2, 3\}$ ,  $J$  is an option in the set  $\{1, 2, 3\}$ ,  $K$  is an option in the set  $\{1, 2, 3\}$  that is neither  $I$  nor  $J$ ,  $L$  is an option in the set  $\{2, 3\}$  that is not  $I$ , and  $M$  is an option in the set  $\{1, 2, 3\}$  that is not  $L$ . Each CDF is obtained by applying (6) to the respective advantage accumulator, and each PDF is obtained by applying (8) to the respective advantage accumulator.

For a decision trial with three response options (i.e., 1, 2, and 3), (10) can be expanded

as:

$$\begin{aligned}
p_1(t) = & \sum_{J \neq 2} \left( PDF_{J-2}(t) \times \prod_{K \neq 2, J} CDF_{K-2}(t) \times \prod_{L \neq 2, 1} \prod_{M \neq L} CDF_{M-L}(t) \right) \times \left( 1 - \prod_{I \neq 1} CDF_{I-1}(t) \right) + \\
& \sum_{J \neq 3} \left( PDF_{J-3}(t) \times \prod_{K \neq 3, J} CDF_{K-3}(t) \times \prod_{L \neq 3, 1} \prod_{M \neq L} CDF_{M-L}(t) \right) \times \left( 1 - \prod_{I \neq 1} CDF_{I-1}(t) \right) \quad (11)
\end{aligned}$$

where  $I$  and  $L$  are options in the set  $\{2, 3\}$ ,  $J$  is an option in the set  $\{1, 2, 3\}$ ,  $K$  is an option in the set  $\{1, 2, 3\}$  that is not  $J$ , and  $M$  is an option in the set  $\{1, 2, 3\}$  that is not  $L$ . The first line represents the sum of all scenarios of  $J$  where accumulator  $J-2$ , where  $J$  is not 2, is the terminating accumulator that prompts the response ( $PDF_{J-2}(t)$ ), all accumulators  $K-2$ , where  $K$  is not 2 or  $J$ , had finished before ( $\prod_{K \neq 2, J} CDF_{K-2}(t)$ ), all accumulators out of the set  $\{1-3, 2-3\}$  had finished before ( $\prod_{L \neq 2, 1} \prod_{M \neq L} CDF_{M-L}(t)$ ), and at least one accumulator out of the set  $\{2-1, 3-1\}$  had not yet finished ( $1 - \prod_{I \neq 1} CDF_{I-1}(t)$ ).

Similarly, the second line represents the sum of all scenarios of  $J$  where accumulator  $J-3$ , where  $J$  is not 3, is the terminating accumulator that prompts the response ( $PDF_{J-3}(t)$ ), all accumulators  $K-3$ , where  $K$  is not 3 or  $J$ , had finished before ( $\prod_{K \neq 3, J} CDF_{K-3}(t)$ ), all accumulators out of the set  $\{1-2, 3-2\}$  had finished before ( $\prod_{L \neq 3, 1} \prod_{M \neq L} CDF_{M-L}(t)$ ), and at least one accumulator out of the set  $\{2-1, 3-1\}$  had not yet finished ( $1 - \prod_{I \neq 1} CDF_{I-1}(t)$ ).

The PDF for response 1 is completed by summing the expressions on both of these lines.

### A3. Lose-One Stopping Rule

The Lose-One model assumes that the decision maker responds as soon as all but one of the response options have been beaten by at least one contrasting alternative. That is, the decision maker chooses 1 from three response options (i.e., 1, 2, and 3) if and only if

1. At least one of the accumulators in each of the sets  $\{1-2, 3-2\}$ , and  $\{1-3, 2-3\}$  have reached their threshold, and:
2. None of the accumulators in the set  $\{2-1, 3-1\}$  has reached their threshold.

Specifically, response option 1 is the last remaining option which has not been beaten by any competitor (another version of “last man standing”). Two layers of counters are required to instantiate this stopping rule. Three counters in the first layer take input from the sets of two just described, each requiring only one count to be triggered. Three counters in the second layer each correspond to a response. They take inputs from two counters in the previous layer (e.g. the counter corresponding to the 1 response takes inputs from the two sets in (1) above), and require two counts to trigger their response.

An advantage of this model is that it cannot produce sequences in which the winning response has ever lost in a direct comparison. However, it is possible to respond 1 without any accumulator that favors 1 having reached threshold (e.g., the sequence  $2-3, 3-2$  will trigger a response 1). Again, with sensible drift rates, this set of events is exceedingly unlikely.

The probability density function for the distribution of responses 1 at time  $t$  is given by

$$p_1(t) = \sum_{I \neq 1} \left[ \sum_{J \neq I} \left( PDF_{J-I}(t) \times \prod_{K \neq I, J} [1 - CDF_{K-I}(t)] \times \prod_{L \neq I, 1} \left[ 1 - \prod_{M \neq L} [1 - CDF_{M-L}(t)] \right] \right) \right] \times \prod_{I \neq 1} [1 - CDF_{I-1}(t)] \quad (12)$$

$I$  is an option in the set  $\{2, 3\}$ ,  $J$  is an option in the set  $\{1, 2, 3\}$ ,  $K$  is an option in the set  $\{1, 2, 3\}$  that is neither  $I$  nor  $J$ ,  $L$  is an option in the set  $\{2, 3\}$  that is not  $I$ , and  $M$  is an option in the set  $\{1, 2, 3\}$  that is not  $L$ . Each CDF is obtained by applying (6) to the respective advantage accumulator, and each PDF is obtained by applying (8) to the respective advantage accumulator.

For a decision trial with three response options (i.e., 1, 2, and 3), (12) can be expanded as:

$$p_1(t) = \sum_{J \neq 2} \left( PDF_{J-2}(t) \times \prod_{K \neq 2, J} [1 - CDF_{K-2}(t)] \times \prod_{L \neq 2, 1} \left[ 1 - \prod_{M \neq L} [1 - CDF_{M-L}(t)] \right] \right) \times \prod_{I \neq 1} [1 - CDF_{I-1}(t)] + \sum_{J \neq 3} \left( PDF_{J-3}(t) \times \prod_{K \neq 3, J} [1 - CDF_{K-3}(t)] \times \prod_{L \neq 3, 1} \left[ 1 - \prod_{M \neq L} [1 - CDF_{M-L}(t)] \right] \right) \times \prod_{I \neq 1} [1 - CDF_{I-1}(t)] \quad (13)$$

where  $I$  and  $L$  are options in the set  $\{2, 3\}$ ,  $J$  is an option in the set  $\{1, 2, 3\}$ ,  $K$  is an option in the set  $\{1, 2, 3\}$  that is not  $J$ , and  $M$  is an option in the set  $\{1, 2, 3\}$  that is not  $L$ . The first line represents the sum of all scenarios of  $J$  where accumulator  $J - 2$ , where  $J$  is not 2, is the terminating accumulator that prompts the response ( $PDF_{J-2}(t)$ ), all accumulators  $K - 2$ , where  $K$  is not 2 or  $J$ , had not yet finished ( $\prod_{K \neq 2, J} [1 - CDF_{K-2}(t)]$ ), at least one accumulator out of the set  $\{1 - 3, 2 - 3\}$  had finished before ( $\prod_{L \neq 2, 1} [1 - \prod_{M \neq L} [1 - CDF_{M-L}(t)]]$ ), and no accumulator out of the set  $\{2 - 1, 3 - 1\}$  had finished yet ( $\prod_{I \neq 1} [1 - CDF_{I-1}(t)]$ ).

Similarly, the second line represents the sum of all scenarios of  $J$  where accumulator  $J - 3$ , where  $J$  is not 3, is the terminating accumulator that prompts the response ( $PDF_{J-3}(t)$ ), all accumulators  $K - 3$ , where  $K$  is not 3 or  $J$ , had not yet finished ( $\prod_{K \neq 3, J} [1 - CDF_{K-3}(t)]$ ), at least one accumulator out of the set  $\{1 - 2, 3 - 2\}$  had finished before ( $\prod_{L \neq 3, 1} [1 - \prod_{M \neq L} [1 - CDF_{M-L}(t)]]$ ), and no accumulator out of the set  $\{2 - 1, 3 - 1\}$  had finished yet ( $\prod_{I \neq 1} [1 - CDF_{I-1}(t)]$ ).

The PDF for response 1 is completed by summing the expressions on both of these lines.

## Appendix B

## Estimation Details

**B1. Estimation Details: Absolute versus Relative Input Differences**

The model was fit to each participant’s data separately using Bayesian Markov-chain Monte Carlo methods in R with the DMC software (Heathcote et al., in press).<sup>5</sup> All scripts, RData files, and plotting code of these and subsequent fits are available on <https://osf.io/2s6ax/files/>.

Vague normal priors were used, truncated at zero for all parameters except  $t_0$ , which was bounded between 0.1s and 1s, with the following means:  $A = 25$ ,  $B_R = 1$ ,  $v_0 = 5$ ,  $w_S = 5$ ,  $w_D = 100$ ,  $s = 5$ , and  $t_0 = 0.3$ . Prior standard deviations had the same values, except for  $t_0$ , where it was 0.2. After burn in, 21 chains of 500 samples, thinned to retain every 10<sup>th</sup> sample, were used for analysis, with convergence supported by multivariate scale-reduction factors (Brooks & Gelman, 1998) of less than 1.01 in all cases, and confirmed visually, as was dominance of the posterior by the prior.

**B2. Estimation Details: Strong versus Weak Distractors**

We estimated parameters for a hierarchical version of the Win-All model using a differential evolution Markov-chain Monte Carlo procedure (ter Braak, 2006; Turner, Sederberg, Brown, & Steyvers, 2013).

Starting values for the MCMC chains for individual parameters were drawn from the following distributions:  $B \sim N(0.5, 0.05)|(0, )$ ,  $A \sim N(1, 0.1)|(0, )$ ,  $t_0 \sim N(0.2, 0.02)|(0, )$ ,  $v_0 \sim N(1, 0.1)|(0, )$ ,  $w_S \sim N(1, 0.1)|(0, )$ , and  $w_D \sim N(1, 0.1)|(0, )$ .

Priors for all group level mean parameters were normal distributions, with  $B_\mu \sim N(0.5, 0.2)|(0, )$ ,  $A_\mu \sim N(1, 0.5)|(0, )$ ,  $t_{0\mu} \sim N(0.2, 0.1)|(0, )$ ,  $v_{0\mu} \sim N(1, 0.5)|(0, )$ ,  $w_{S\mu} \sim N(1, 0.5)|(0, )$ , and  $w_{D\mu} \sim N(1, 0.5)|(0, )$ . Priors for all group level standard deviation parameters were exponential distributions with a mean of 1. Starting values for the MCMC chains for group level  $\mu$  parameters were drawn from the same distributions as those for the individual parameters, and starting values for group level  $\sigma$  parameters were derived from starting value distributions for the individual parameters by dividing the mean by 10 and the standard deviation by 2.

For sampling, we used 32 interacting Markov chains for all runs, and ran each for 1,000 burn-in iterations followed by 1,000 iterations after convergence. The two tuning parameters of the differential evolution proposal algorithm were set to standard values used in previous work: random perturbations were added to all proposals drawn uniformly from the interval  $[-.001, .001]$ ; and the scale of the difference added for proposal generation was set to  $\gamma = 2.38 \times (2K)^{-0.5}$ , where  $K$  is the number of parameters per participant. The MCMC chains blocked proposals separately for each participant’s parameters, and also blocked the group-level parameters in  $\{\mu, \sigma\}$  pairs.

Following burn-in, sampling chains that were at least 3 across-chain standard deviations removed from the mean were reset to the mean in an iterative procedure for each estimated parameter (2.6% of all chains were reset this way). Parameter con-

<sup>5</sup>We provide an RStudio project containing the data, DMC functions, and scripts to fit and check the model as a special case of a more general modeling framework that allows a power transformation of objective to subjective values and for rate variability to increase with the mean rate.

vergence was assessed visually and considered satisfactory (trace plots are available on <https://osf.io/2s6ax/files/>).

### B3. Estimation Details: Hick’s Law

We used the same Bayesian hierarchical estimation methods as in the previous section. Again, following burn-in, each parameter chain that was at least 3 across-chain standard deviations removed from the mean was reset to the mean in an iterative procedure (2.8% of all chains were reset this way). Parameter convergence was assessed visually and considered satisfactory (trace plots are available on <https://osf.io/2s6ax/files/>).

Starting values for the MCMC chains for individual parameters were drawn from the following distributions:  $B \sim N(0.5, 0.05)|(0, )$ ,  $A \sim N(2, 0.2)|(0, )$ ,  $t_0 \sim N(0.25, 0.025)|(0, )$ ,  $v_0 \sim N(1, 0.1)|(0, )$ ,  $w_S \sim N(0.5, 0.05)|(0, )$ ,  $w_D \sim N(6, 0.6)|(0, )$ ,  $\beta \sim N(0.1, 0.01)|(0, )$ , and  $\log(\alpha) \sim N(0, 0.3)|(-3, )$ .

Priors for all group level mean parameters were normal distributions, with  $B_\mu \sim N(0.5, 0.25)|(0, )$ ,  $A_\mu \sim N(2, 1)|(0, )$ ,  $t_{0\mu} \sim N(0.25, 0.1)|(0, )$ ,  $v_{0\mu} \sim N(1, 0.5)|(0, )$ ,  $w_{S\mu} \sim N(0.5, 0.25)|(0, )$ ,  $w_{D\mu} \sim N(6, 3)|(0, )$ ,  $\beta_\mu \sim N(0.1, 0.05)|(0, )$ , and  $\log(\alpha_\mu) \sim N(3, 1)|(-3, )$ . Priors for all group level standard deviation parameters were exponential distributions with a mean of 1. Starting values for the MCMC chains for group level  $\mu$  parameters were drawn from the same distributions as those for the individual parameters, and starting values for group level  $\sigma$  parameters were derived from starting value distributions for the individual parameters by dividing the mean by 10 and the standard deviation by 2.

For sampling, we used 32 interacting Markov chains for all runs, and ran each for 2,000 burn-in iterations followed by 2,000 iterations after convergence. The two tuning parameters of the differential evolution proposal algorithm were set to standard values used in previous work: random perturbations were added to all proposals drawn uniformly from the interval  $[-.001, .001]$ ; and the scale of the difference added for proposal generation was set to  $\gamma = 2.38 \times (2K)^{-0.5}$ , where  $K$  is the number of parameters per participant. The MCMC chains blocked proposals separately for each participant’s parameters, and also blocked the group-level parameters in  $\{\mu, \sigma\}$  pairs.

## Appendix C

### Parameter Recovery

#### C1. Parameter Recovery Strong versus Weak Distractors

Parameter Recovery was performed by generating data from the median parameter estimates of a Win-All fit to the Teodorescu et al. (2016) data set. The Win-All model with the same parameter constraints that were used on the empirical data set was then fit to this generated data set. The resulting parameter estimates (95% credible interval in parentheses) were then compared to the true parameters. Parameter recovery was excellent, details are shown in Table C1.

#### C2. Parameter Recovery Hick’s Law

Parameter Recovery was performed by generating data from the median parameter estimates of the ALBA-1 fit to the van Maanen data set. The resulting parameter esti-

Table C1

*Estimated parameters of the ALBA model for the generated Teodorescu data set. Displayed are the true parameter values, with a 95% credible interval of the posterior for the recovered parameters presented in parentheses. Columns represent parameters and rows represent different participants (hyper = parameters of the group-level distributions).*

Pp	$B$	$A$	$t_0$	$v_0$	$w_S$	$w_D$
<b>Hyper</b>	<b>0.18 (0.03, 0.44)</b>	<b>1.03 (0.23, 1.83)</b>	<b>0.51 (0.16, 0.62)</b>	<b>1.26 (0.61, 2.14)</b>	<b>0.17 (0.06, 0.79)</b>	<b>1.61 (0.36, 2.97)</b>
1	0.07 (0.06, 0.35)	0.88 (0.72, 0.95)	0.65 (0.58, 0.66)	1.41 (1.43, 2.62)	0.21 (0.09, 0.62)	3.28 (2.48, 3.20)
2	0.11 (0.07, 0.40)	1.12 (0.97, 1.33)	0.67 (0.58, 0.68)	1.08 (1.04, 12.11)	0.29 (0.18, 4.21)	3.84 (2.30, 4.48)
3	0.01 (0.00, 0.08)	0.59 (0.54, 0.70)	0.64 (0.61, 0.64)	1.58 (1.45, 8.97)	0.20 (0.04, 2.75)	3.07 (1.48, 3.17)
4	0.12 (0.01, 0.42)	4.08 (3.39, 4.32)	0.47 (0.37, 0.52)	1.31 (1.36, 2.70)	0.10 (0.21, 0.84)	3.65 (3.50, 4.24)
5	0.43 (0.09, 0.43)	1.19 (1.02, 1.35)	0.57 (0.57, 0.66)	1.50 (0.83, 2.40)	0.25 (0.16, 1.13)	4.09 (4.31, 5.78)
6	0.63 (0.24, 0.94)	1.86 (1.77, 2.30)	0.61 (0.53, 0.68)	1.86 (1.86, 3.31)	0.06 (0.05, 0.74)	3.51 (3.22, 4.01)
7	0.39 (0.17, 0.77)	2.34 (2.27, 2.92)	0.59 (0.49, 0.63)	1.67 (1.34, 2.39)	0.23 (0.01, 0.48)	3.88 (3.41, 4.25)
8	0.01 (0.03, 0.28)	0.91 (0.81, 1.05)	0.64 (0.55, 0.63)	1.05 (0.61, 1.95)	0.46 (0.14, 0.75)	4.01 (3.12, 4.15)

Table C2

*Estimated parameters of the ALBA- $\beta$  model for the generated van Maanen data set. Displayed are the true parameter values, with a 95% credible interval of the posterior for the recovered parameters presented in parentheses. Columns represent parameters and rows represent different participants (hyper = parameters of the group-level distributions).*

Pp	$B$	$A$	$t_0$	$v_0$	$w_S$	$w_D$	$\alpha$
<b>Hyper</b>	<b>0.11 (0.01, 0.34)</b>	<b>1.16 (1.02, 1.27)</b>	<b>0.35 (0.21, 0.39)</b>	<b>0.21 (0.03, 0.90)</b>	<b>0.41 (0.03, 0.68)</b>	<b>11.66 (4.81, 12.78)</b>	<b>0.15 (0.07, 0.50)</b>
1	0.11 (0.11, 0.34)	1.22 (1.00, 1.21)	0.33 (0.26, 0.36)	0.13 (0.01, 0.47)	0.13 (0.01, 0.27)	10.21 (6.46, 15.28)	0.14 (0.09, 0.22)
2	0.05 (0.02, 0.14)	1.14 (1.03, 1.19)	0.37 (0.33, 0.39)	0.32 (0.04, 0.85)	0.27 (0.02, 0.45)	16.56 (9.86, 25.10)	0.09 (0.06, 0.15)
3	0.14 (0.07, 0.25)	1.25 (1.12, 1.33)	0.30 (0.26, 0.34)	0.12 (0.01, 0.39)	0.11 (0.00, 0.20)	12.17 (6.91, 14.06)	0.15 (0.13, 0.29)
4	0.05 (0.01, 0.12)	1.03 (1.01, 1.17)	0.33 (0.29, 0.34)	0.28 (0.06, 1.10)	0.42 (0.02, 0.59)	14.88 (10.28, 22.82)	0.09 (0.06, 0.14)
5	0.19 (0.16, 0.37)	1.19 (1.11, 1.27)	0.43 (0.38, 0.44)	0.20 (0.08, 1.17)	1.12 (0.64, 1.25)	4.49 (3.17, 5.06)	0.38 (0.32, 0.55)

mates (95% credible interval in parentheses) were then compared to the true parameters. Parameter recovery was excellent, details are shown in Table C2.

## Appendix D Additional Fits

### D1. Additional Fits Strong versus Weak Distractors

The posterior predictive data for the WA fit with rate variability  $s$  free to vary are shown in Figure D1. Figure D1 shows that this model fits the data well, but offers no qualitative improvement over the model with rate variability  $s$  constrained between conditions.

The posterior predictive data for the LBA fit can be found in Figure D2. Figure D2 shows that this model fits the RT data well, but overestimates error rates in both conditions.

### D2. Additional Fits Hick's Law

The posterior predictive data for the Win-All version of the ALBA model with parameter  $B$  free to vary with set-size conditions can be found in Figure D3. Figure D3 shows that relaxing  $B$  to vary across set-sizes does not yield a noticeable improvement over the more constrained model, it cannot pick up the increasing error rates for higher set-sizes.

The posterior predictive data for the Win-All version of the ALBA model with parameter  $A$  free to vary with set-size conditions can be found in Figure D4. Figure D4 shows

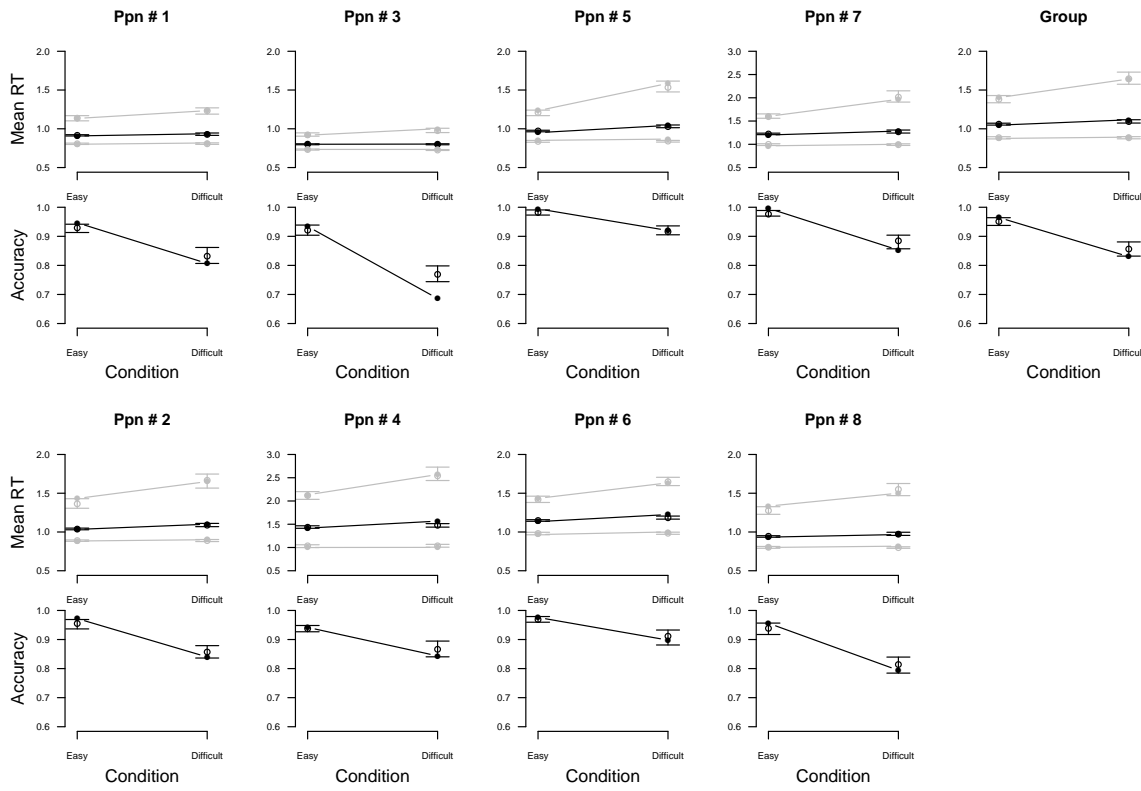


*Figure D1.* Posterior predictive data for fits to the Experiment 1A data of Teodorescu and Usher (2013) with rate variability  $s$  free to vary between the two conditions. RTs for the .5 (black), .1, and .9 (gray) deciles calculated for the easy (top-left) and difficult (top-right) condition, and the proportion of correct responses for the easy (bottom-left) and difficult (bottom-right) condition, both at the individual level (left four columns) and for aggregate data (right column). For all panels, error bars represent posterior predictive data simulated from model fits (the bar extends to the middle 95% of generated summary statistics, with the dot in the middle indicating the median) and lines represent data. See text for details.

that relaxing  $A$  to vary across set-sizes does not yield a noticeable improvement over the more constrained model, it cannot pick up the increasing error rates for higher set-sizes.

The posterior predictive data for the Win-All version of the ALBA model with parameters  $B$  and  $A$  free to vary with set-size conditions can be found in Figure D5. Figure D5 shows that relaxing both  $B$  and  $A$  allows the model to pick up both the RT and proportion correct data fairly well. Compared to the model that varies rate variability  $S$  presented in the main text, the model with  $B$  and  $A$  free to vary struggles to pick up proportion correct data for set-size 3 and struggles to capture some of the slower RT quantiles.

The posterior predictive data for the LBA fit can be found in Figure D6. Figure D6 shows that this model fits the RT data well, but overestimates the increase in error rates for higher set-sizes.



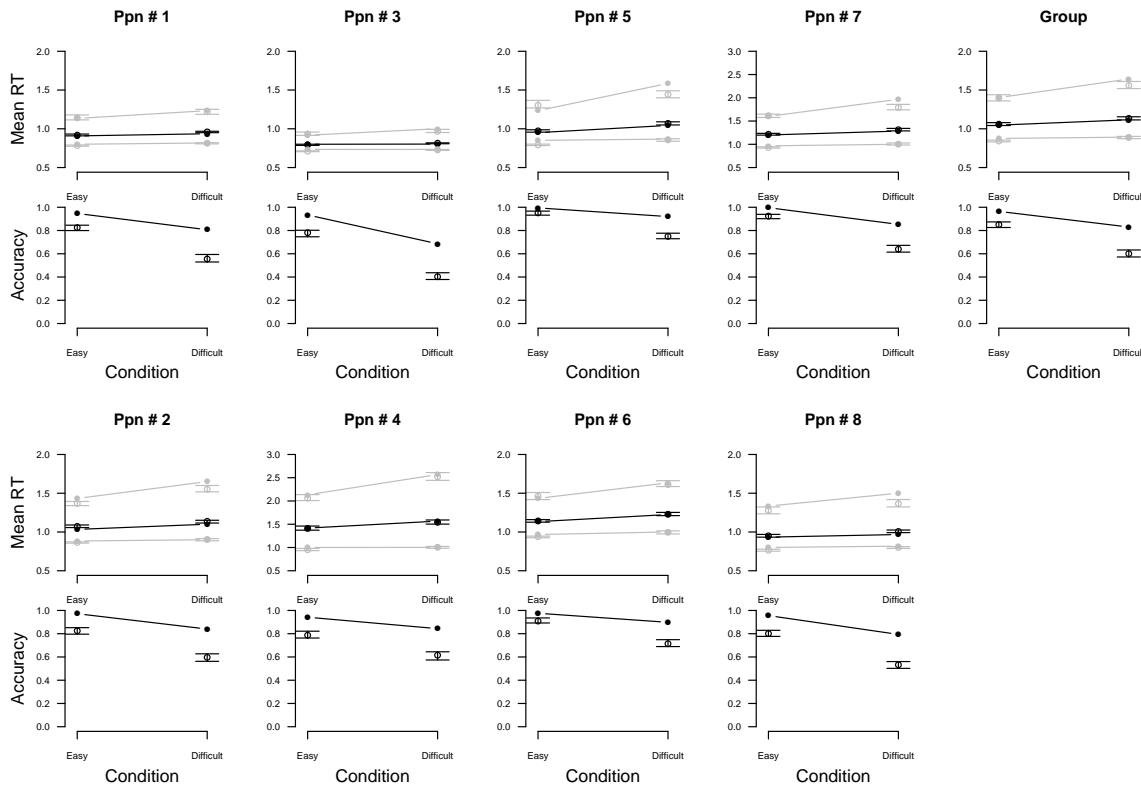


*Figure D2.* LBA posterior predictive data for the Teodorescu data. RTs for the .1, .5, and .9 deciles (top) and the proportion of correct responses (bottom) as a function of set-size ( $N$ ) on a logarithmic scale. Posterior predictives are presented at the individual level and for aggregate data (bottom-right panel). For all panels, box-and-whiskers represent posterior predictive data (the box contains 95% of the simulated data, with a bar across the middle indicating the median, and whiskers extend to the data extremes) and lines represent data. See text for details.

## Appendix E Context Effects

Here, we show that the ALBA can produce two multiattribute context effects: the attraction effect (Huber et al., 1982) (also called the asymmetric dominance effect) and the compromise effect (Simonson, 1989). Both effects are about two stimuli,  $S_1$  and  $S_2$ , that differ on two attributes,  $A_1$  and  $A_2$ .  $S_1$  is preferable on  $A_1$ , but  $S_2$  is preferable on  $A_2$ , such that in a binary choice  $S_1$  and  $S_2$  are indifferent. The attraction effect occurs when a third stimulus,  $S_3$ , is introduced that is slightly inferior to  $S_1$  on both  $A_1$  and  $A_2$ , resulting in a preference for  $S_1$  over  $S_2$ . The compromise effect occurs when a third stimulus,  $S_3$ , is introduced that is even more preferable on  $A_1$  and even less preferable on  $A_2$  than  $S_1$ , resulting in a preference for  $S_1$ , the intermediate option.

The purpose of this section is not for ALBA to provide a detailed account of the attraction and compromise effects. Researchers interested in capturing these phenomena

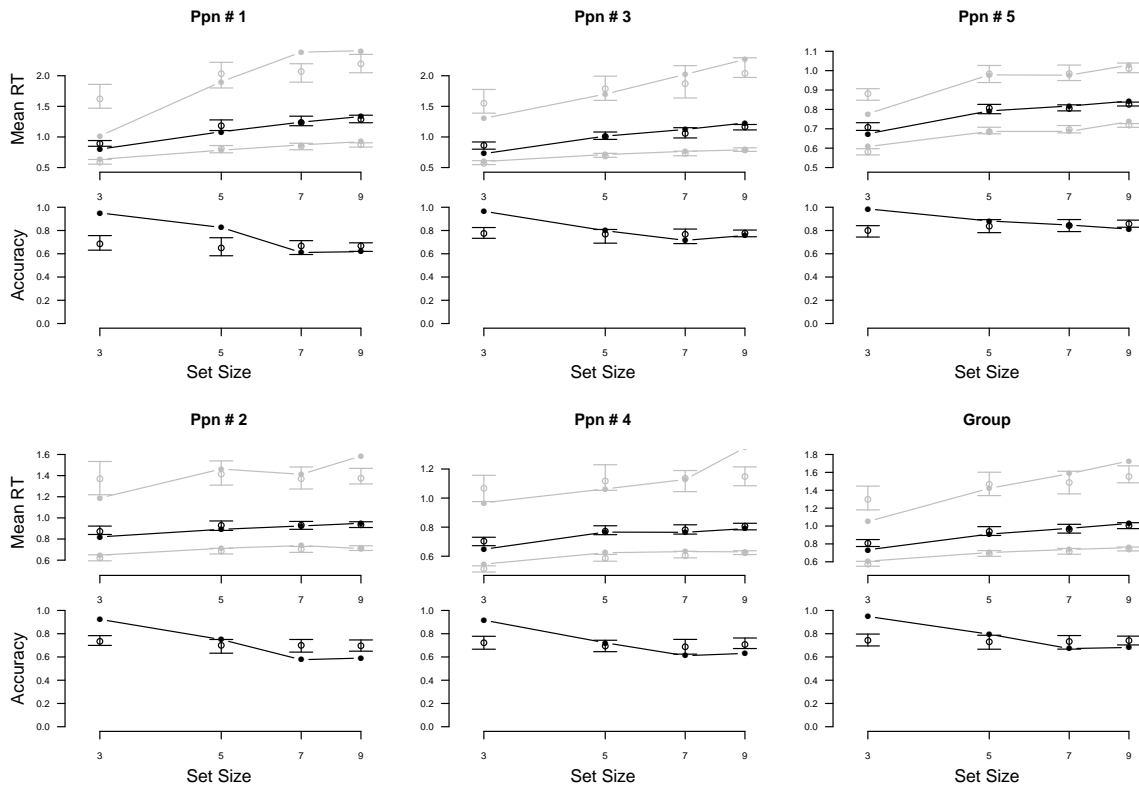


*Figure D3.* Posterior predictive data for the ALBA-4B fit to the van Maanen data. RTs for the .5 (black), .1, and .9 (gray) deciles (top) and the proportion of correct responses (bottom) as a function of set-size ( $N$ ) on a logarithmic scale. Posterior predictives are presented at the individual level and for aggregate data (bottom-right panel). For all panels, box-and-whiskers represent posterior predictive data (the box contains 95% of the simulated data, with a bar across the middle indicating the median, and whiskers extend to the data extremes) and lines represent data. See text for details.

should use a specialized model like the one developed by Trueblood et al. (2014). Rather, this section intends to showcase how the architecture of ALBA is such that it can produce these qualitative effects naturally.

For this simulation, context effects were modeled as follows. All three effects were examined using two basic stimuli that varied on two attributes: Stimulus 1 had subjective input values  $\{4, 6\}$  for attributes 1 and 2 respectively, stimulus 2 had subjective input values  $\{6, 4\}$  for attributes 1 and 2 respectively. For the attraction and compromise effects, we investigated the consequences of adding an extra stimulus to this pair.

For the attraction effect, the extra stimulus (“3”) had subjective input values  $\{3, 6\}$  for attributes 1 and 2 respectively. The attraction effect posits that the presence of stimulus 3 should lead decision makers to prefer stimulus 1, because stimulus 1 “dominates” stimulus 3.

For the compromise effect, the extra stimulus (“4”) had subjective input values  $\{2,$

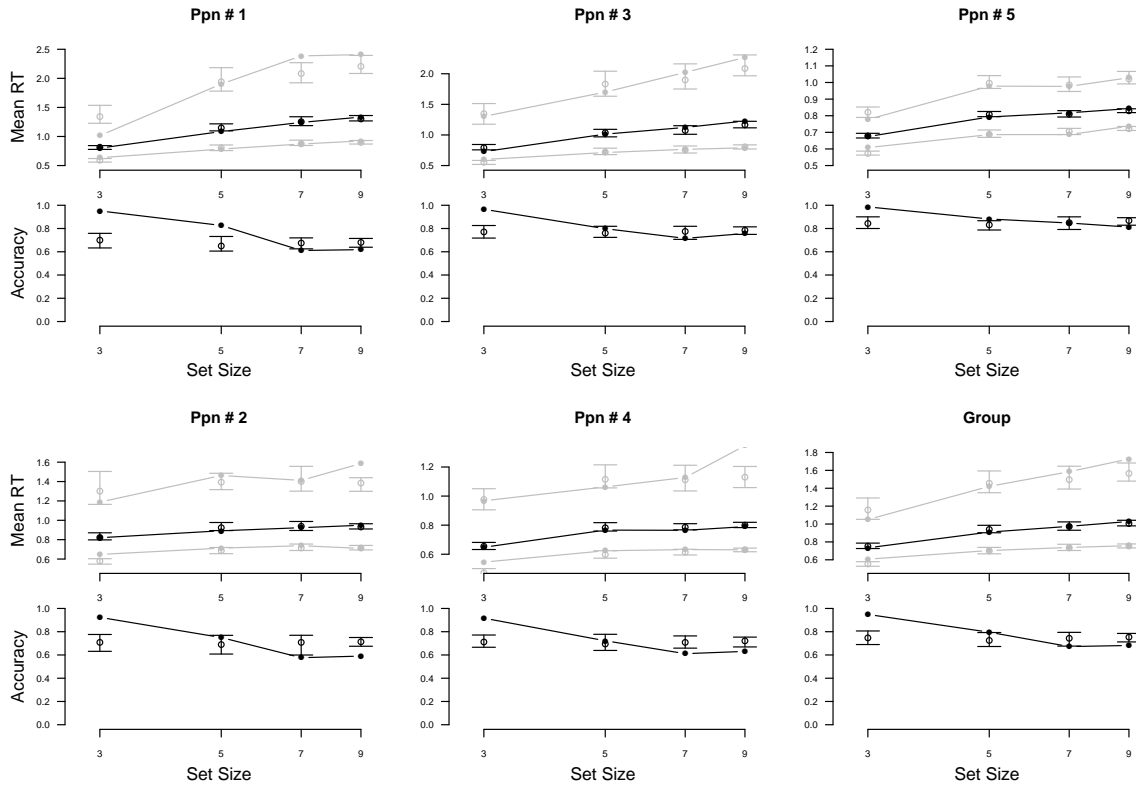


Figure D4. Posterior predictive data for the ALBA-4A fit to the van Maanen data. RTs for the .5 (black), .1, and .9 (gray) deciles (top) and the proportion of correct responses (bottom) as a function of set-size (N) on a logarithmic scale. Posterior predictives are presented at the individual level and for aggregate data (bottom-right panel). For all panels, box-and-whiskers represent posterior predictive data (the box contains 95% of the simulated data, with a bar across the middle indicating the median, and whiskers extend to the data extremes) and lines represent data. See text for details.

8} for attributes 1 and 2 respectively. The compromise effect posits that the presence of stimulus 4 should lead decision makers to prefer stimulus 1, because it is a compromise between stimuli 2 and 4.

Both effects were simulated in the ALBA by modeling two separate ALBA processes, one for attribute 1 and one for attribute 2. A decision was made once the stopping rule was satisfied for both processes. For instance, for a Win-All stopping rule, stimulus 1 needed to beat the other stimuli on both attribute 1 and attribute 2 before a response in favor of stimulus 1 was executed.

For every effect and each model, we ran 10,000 individual simulations. Individual parameters were  $B = 0.2$ ,  $A = 1$ ,  $t_0 = 0.5$ ,  $v_0 = 1.3$ ,  $w_S = 0.2$ , and  $w_D = 3.5$ . Results of the simulations are presented in Table E1. The table presents the proportion of times each of the three stimuli was chosen.

The probability of choosing stimulus 1 (resp., 2) from the set {1, 2} is 1/2 (resp., 1/2).

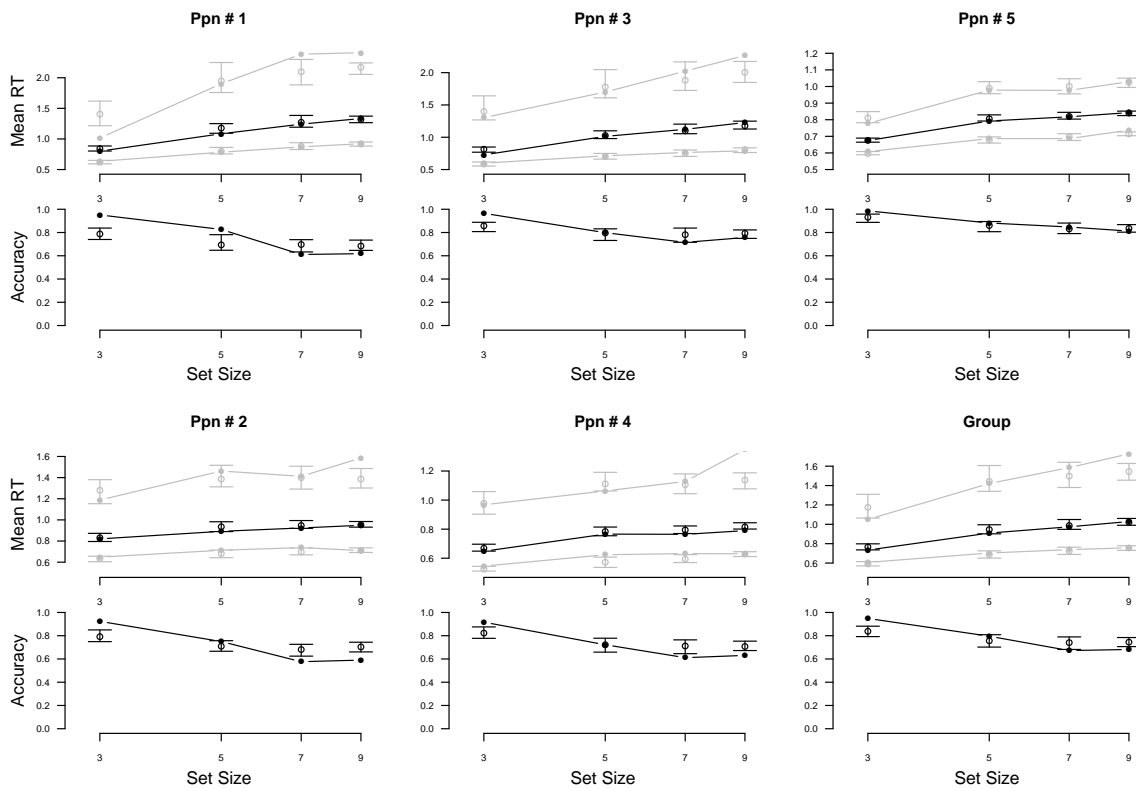


Figure D5. Posterior predictive data for the ALBA-4BA fit to the van Maanen data. RTs for the .5 (black), .1, and .9 (gray) deciles (top) and the proportion of correct responses (bottom) as a function of set-size (N) on a logarithmic scale. Posterior predictives are presented at the individual level and for aggregate data (bottom-right panel). For all panels, box-and-whiskers represent posterior predictive data (the box contains 95% of the simulated data, with a bar across the middle indicating the median, and whiskers extend to the data extremes) and lines represent data. See text for details.

The attraction effect is shown by the fact that the probability that stimulus 1 is chosen from the set {1, 2, 3} is greater than one half, and the compromise effect is shown by the fact that stimulus 1 is chosen from the set {1, 2, 4} more often than either stimulus stimulus 2 or stimulus 4.

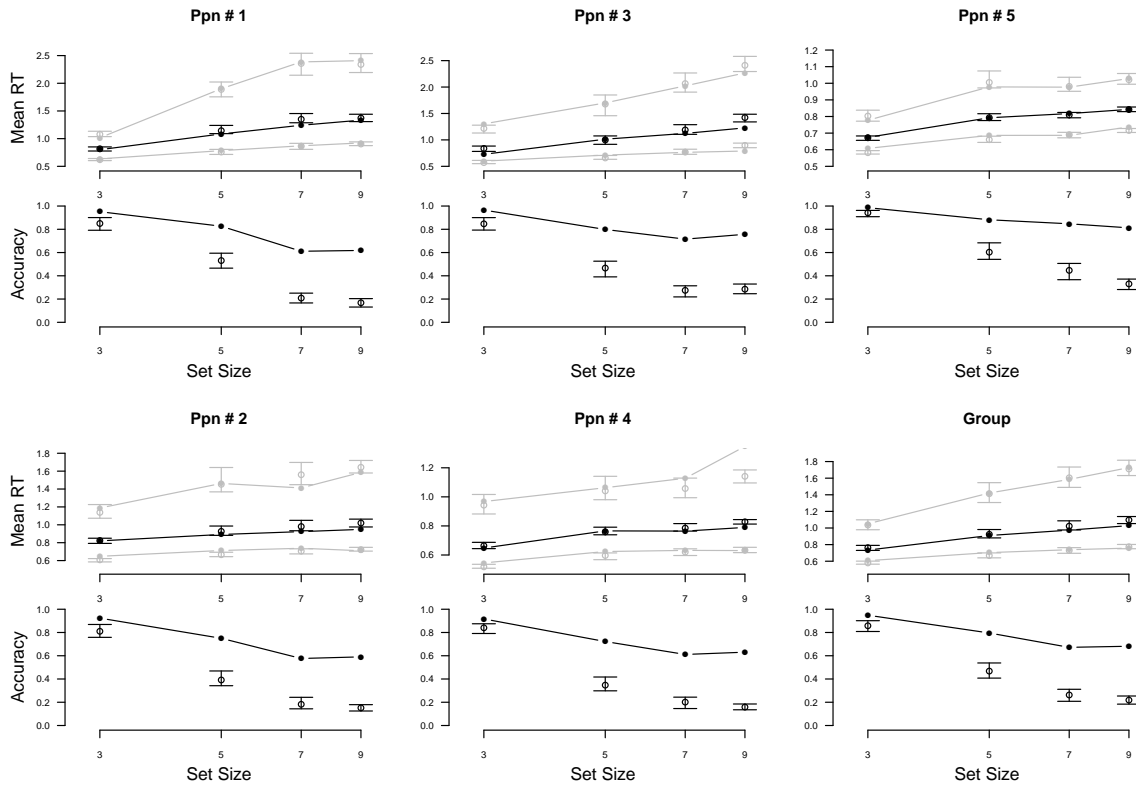


Figure D6. LBA posterior predictive data for the van Maanen data. RTs for the .1, .5, and .9 deciles (top) and the proportion of correct responses (bottom) as a function of set-size (N) on a logarithmic scale. Posterior predictives are presented at the individual level and for aggregate data (bottom-right panel). For all panels, box-and-whiskers represent posterior predictive data (the box contains 95% of the simulated data, with a bar across the middle indicating the median, and whiskers extend to the data extremes) and lines represent data. See text for details.

Table E1

Attraction and compromise effects, as indicated by the proportion of times stimulus 1 was chosen. Attribute values for stimulus 3 for the attraction effect are displayed with attribute values for the compromise effect in parentheses. The most common choice is printed bold.

Stimulus	Attribute 1	Attribute 2	Attraction	Compromise
1	4	6	<b>0.51</b>	<b>0.57</b>
2	6	4	0.30	0.32
3	3	6	0.19	—
3	2	8	—	0.11

## References

- Blavatsky, P. (2012). Probabilistic choice and stochastic dominance. *Economic Theory*, *50*, 59 – 83.
- Bogacz, R., Usher, M., Zhang, J., & McClelland, J. L. (2007). Extending a biologically inspired model of choice: Multi-alternatives, nonlinearity and value-based multidimensional choice. *Philosophical Transactions of the Royal Society, Series B*, *362*, 1655–1670.
- Britten, K. H., Shadlen, M. N., Newsome, W. T., & Movshon, J. A. (1992). The analysis of visual motion: A comparison of neuronal and psychophysical performance. *Journal of Neuroscience*, *12*, 4745–4765.
- Brooks, S. P., & Gelman, A. (1998). General methods for monitoring convergence of iterative simulations. *Journal of computational and graphical statistics*, *7*(4), 434–455.
- Brown, S. D., & Heathcote, A. (2005). A ballistic model of choice response time. *Psychological Review*, *112*, 117–128.
- Brown, S. D., & Heathcote, A. (2008). The simplest complete model of choice reaction time: Linear ballistic accumulation. *Cognitive Psychology*, *57*, 153–178.
- Brown, S. D., Marley, A. A. J., Donkin, C., & Heathcote, A. (2008a). An integrated model of choices and response times in absolute identification. *Psychological Review*, *115*, 396–425.
- Brown, S. D., Marley, A. A. J., Donkin, C., & Heathcote, A. (2008b). An integrated model of choices and response times in absolute identification. *Psychological Review*, *115*(2), 396–425.
- Brown, S. D., Steyvers, M., & Wagenmakers, E.-J. (2009). Observing evidence accumulation during multi-alternative decisions. *Journal of Mathematical Psychology*, *53*, 453–462.
- Busemeyer, J. R., Townsend, J. T., Diederich, A., & Barkan, R. (2005). Contrast effects or loss aversion? Comment on Usher and McClelland (2004). *Psychological Review*, *112*, 253–255.
- Dassonville, P., Lewis, S. M., Foster, H. E., & Ashe, J. (1999). Choice and stimulus-response compatibility affect duration of response selection. *Cognitive Brain Research*, *7*, 235–240.
- Donkin, C., Brown, S. D., & Heathcote, A. (2009). The overconstraint of response time models: Rethinking the scaling problem. *Psychonomic Bulletin & Review*, *16*(6), 1129–1135.
- Eidels, A., Donkin, C., Brown, S. D., & Heathcote, A. (2010). Converging measures of workload capacity. *Psychonomic bulletin & review*, *17*(6), 763–771.
- Fechner, G. T., Boring, E. G., Howes, D. H., & Adler, H. E. (1966). *Elements of psychophysics*. Holt, Rinehart and Winston.
- Hawkins, G. E., Brown, S. D., Steyvers, M., & Wagenmakers, E.-J. (2012a). Context effects in multi-alternative decision making: Empirical data and a Bayesian model. *Cognitive Science*, *36*, 498–516.
- Hawkins, G. E., Brown, S. D., Steyvers, M., & Wagenmakers, E.-J. (2012b). An optimal adjustment procedure to minimize experiment time in decisions with multiple alternatives. *Psychonomic Bulletin & Review*, *19*, 339–348.

- Hawkins, G. E., Marley, A. A. J., Heathcote, A., Flynn, T. N., Louviere, J. J., & Brown, S. D. (2014). Integrating cognitive process and descriptive models of attitudes and preferences. *Cognitive Science*, *38*, 701–735.
- Heathcote, A., Lin, Y.-S., Reynolds, A., Strickland, L., Gretton, M., & Matzke, D. (in press). Dynamic models of choice. *Behavior Research Methods*.
- Heathcote, A., & Love, J. (2012). Linear deterministic accumulator models of simple choice. *Frontiers in Psychology*, *3*.
- Heathcote, A., Suraev, A., Curley, S., Gong, Q., & Love, J. (2015). Decision processes and the slowing of simple choices in schizophrenia. *Journal of Abnormal Psychology*, *124*, 961–974.
- Hick, W. E. (1952). On the rate of gain of information. *Quarterly Journal of Experimental Psychology*, *4*, 11–26.
- Holmes, W. R., Trueblood, J. S., & Heathcote, A. (2016). A new framework for modeling decisions about changing information: The piecewise linear ballistic accumulator model. *Cognitive Psychology*, *85*, 1–29.
- Huber, J., Payne, J. W., & Puto, C. (1982). Adding asymmetrically dominated alternatives: Violations of regularity and the similarity hypothesis. *Journal of Consumer Research*, *9*, 90–98.
- Hyman, R. (1953). Stimulus information as a determinant of reaction time. *Journal of Experimental Psychology*, *45*, 188–196.
- Kveraga, K., Boucher, L., & Hughes, H. C. (2002). Saccades operate in violation of Hick's law. *Experimental Brain Research*, *146*, 307–314.
- Lacouture, Y., & Marley, A. A. J. (1995). A mapping model of bow effects in absolute identification. *Journal of Mathematical Psychology*, *39*, 383–395.
- Lee, K.-M., Keller, E. L., & Heinen, S. J. (2005). Properties of saccades generated as a choice response. *Experimental Brain Research*, *162*, 278–286.
- Leite, F. P., & Ratcliff, R. (2010). Modeling reaction time and accuracy of multiple-alternative decisions. *Attention, Perception, & Psychophysics*, *72*, 246–273.
- Luce, R. D. (1986). *Response times*. New York: Oxford University Press.
- Marley, A. A. J. (1991). Context dependent probabilistic choice models based on measures of binary advantage. *Mathematical Social Sciences*, *21*, 201–231.
- McClelland, J. L., Usher, M., & Tsetsos, K. (2011). Testing multi-alternative decision models with non-stationary evidence. *Frontiers in Neuroscience*, *5*, 1662–4548.
- McMillen, T., & Holmes, P. (2006). The dynamics of choice among multiple alternatives. *Journal of Mathematical Psychology*, *50*, 30–57.
- Miletic, S., Turner, B. M., Forstmann, B., & Van Maanen, L. (2017). Parameter Recovery for the Leaky Competing Accumulator Model. *Journal of Mathematical Psychology*, *76*, 25–50.
- Pachella, R. G., & Fisher, D. (1972). Hick's law and the speed-accuracy trade-off in absolute judgment. *Journal of Experimental Psychology*, *92*, 378.
- Raab, D. H. (1962). Statistical facilitation of simple reaction times. *Transactions of the New York Academy of Sciences*, *24*, 574–590.
- Ratcliff, R., Voskuilen, C., & Teodorescu, A. (2018). Modeling 2-alternative forced-choice tasks: Accounting for both magnitude and difference effects. *Cognitive Psychology*, *103*, 1–22.

- Simonson, I. (1989). Choice based on reasons: The case of attraction and compromise effects. *Journal of Consumer Research*, *16*, 158–174.
- Spiegelhalter, D. J., Best, N. G., Carlin, B. P., & van der Linde, A. (2002). Bayesian measures of model complexity and fit. *Journal of the Royal Statistical Society B*, *64*, 583–639.
- Teichner, W. H., & Krebs, M. J. (1974). Laws of visual choice reaction time. *Psychological Review*, *81*, 75–98.
- ten Hoopen, G., Akerboom, S., & Raaymakers, E. (1982). Vibrotactile choice reaction time, tactile receptor systems and ideomotor compatibility. *Acta Psychologica*, *50*, 143–157.
- Teodorescu, A. R., Moran, R., & Usher, M. (2016). Absolutely relative or relatively absolute: Violations of value invariance in human decision making. *Psychonomic Bulletin & Review*, *23*, 22–38.
- Teodorescu, A. R., & Usher, M. (2013). Disentangling decision models: From independence to competition. *Psychological Review*, *120*, 1–38.
- ter Braak, C. J. F. (2006). A Markov chain Monte Carlo version of the genetic algorithm Differential Evolution: easy Bayesian computing for real parameter spaces. *Statistics and Computing*, *16*, 239–249.
- Terry, A., Marley, A. A. J., Barnwal, A., Wagenmakers, E.-J., Heathcote, A., & Brown, S. D. (2015). Generalising the drift rate distributions for Linear Ballistic Accumulators. *Journal of Mathematical Psychology*, *68*, 49–58.
- Trueblood, J. S., Brown, S. D., & Heathcote, A. (2014). The multiattribute linear ballistic accumulator model of context effects in multialternative choice. *Psychological Review*, *121*, 179–205.
- Turner, B. M., Sederberg, P. B., Brown, S. D., & Steyvers, M. (2013). A method for efficiently sampling from distributions with correlated dimensions. *Psychological Methods*, *18*, 368–384.
- Tversky, A., & Simonson, I. (1993). Context-dependent preferences. *Management Science*, *39*, 1179–1189.
- Usher, M., & McClelland, J. L. (2001). On the time course of perceptual choice: The leaky competing accumulator model. *Psychological Review*, *108*, 550–592.
- Usher, M., & McClelland, J. L. (2004). Loss aversion and inhibition in dynamical models of multialternative choice. *Psychological Review*, *111*, 757–769.
- Usher, M., Olami, Z., & McClelland, J. L. (2002). Hick’s Law in a Stochastic Race Model with Speed–Accuracy Tradeoff. *Journal of Mathematical Psychology*, *46*, 704–715.
- van Maanen, L., Grasman, R. P. P. P., Forstmann, B. U., Keuken, M. C., Brown, S. D., & Wagenmakers, E.-J. (2012). Similarity and number of alternatives in the random-dot motion paradigm. *Attention, Perception, & Psychophysics*, *74*, 739–753.
- van Ravenzwaaij, D., van der Maas, H. L. J., & Wagenmakers, E.-J. (2012). Optimal decision making in neural inhibition models. *Psychological Review*, *119*, 201–215.
- Vickrey, C., & Neuringer, A. (2000). Pigeon reaction time, Hick’s law, and intelligence. *Psychonomic Bulletin & Review*, *7*, 284–291.